Zootaxa 5213 (1): 001–035
https://www.mapress.com/zt/

Article

ISSN 1175-5326 (print edition)
ZOOTAXA
ISSN 1175-5334 (online edition)

https://doi.org/10.11646/zootaxa.5213.1.1
http://zoobank.org/urn:lsid:zoobank.org:pub:193AA500-8D45-4E18-BB47-339A916BB11E

Five new species of black coral (Anthozoa; Antipatharia) from the Great Barrier Reef and Coral Sea, Australia

JEREMY HOROWITZ*[1,2], DENNIS OPRESKO[3], TINA N. MOLODTSOVA[4], ROBIN J. BEAMAN[5], PETER F. COWMAN[1,2,6] & TOM C.L. BRIDGE[1,2]

[1]*Australian Research Council Centre of Excellence for Coral Reef Studies, James Cook University, 101 Angus Smith Drive, Townsville, QLD, 4811, Australia.*

[2] *Biodiversity and Geosciences Program, Museum of Tropical Queensland, Queensland Museum, 70-102 Flinders St, Townsville, QLD, 4810, Australia.*

tom.bridge@qm.qld.gov.au; https://orcid.org/0000-0003-3951-284X

[3]*Department of Invertebrate Zoology, National Museum of Natural History, Smithsonian Institution, 10th St. & Constitution Ave. NW, Washington, DC 20560 USA.*

dmopresko@hotmail.com; https://orcid.org/0000-0001-9946-1533

[4] *P.P. Shirshov Institute of Oceanology, 36 Nakhimovsky prt, Moscow, 117997, Russian Federation*

tina@ocean.ru; https://orcid.org/0000-0001-7171-6952

[5] *College of Science and Engineering, James Cook University, Cairns, Queensland 4870, Australia*

robin.beaman@jcu.edu.au; https://orcid.org/0000-0003-3972-9862

[6] *Centre for Tropical Bioinformatics and Molecular Biology, Molecular and Cell Biology, James Cook University, 101 Angus Smith Drive, Townsville, QLD, 4811, Australia*

peter.cowman@qm.qld.gov.au; https://orcid.org/0000-0001-5977-5327

**Corresponding author. jeremy.horowitz@my.jcu.edu.au; https://orcid.org/0000-0002-2643-5200*

Abstract

We describe five new species of black corals from the Great Barrier Reef and Coral Sea, collected at depths ranging from 14 to 789 m: two in the family Antipathidae (*Antipathes falkorae* **sp. nov.** and *Antipathes morrisi* **sp. nov.***),* two in the family Aphanipathidae (*Aphanipathes flailum* **sp. nov.** and *Rhipidipathes helae* **sp. nov.***)*, and one in the family Cladopathidae (*Hexapathes bikofskii* **sp. nov.**). We also present a phylogeny of 80 black corals reconstructed from a target capture dataset of ultraconserved elements and exons, to show the systematic relationships among new and nominal species. This phylogeny also represents a backbone for future species descriptions and research into the evolutionary history of the Antipatharia.

Key words: Hexacorallia, targeted capture, new species, phylogeny, Indo-West Pacific

Introduction

Black corals are an anthozoan order consisting of 296 currently accepted species (WoRMS 2022, accessed April 2022) that are found in most marine habitats, all oceans, and from just below the surface to over 8,000 m depth. Black corals are ecologically important because they provide three-dimensional habitats for other invertebrates (Sánchez 1999; Love *et al.* 2007; Wagner *et al.* 2012; Bo *et al.* 2012), especially in the deep sea where photosymbiotic corals cannot survive. Black corals are threatened because they are slow growing, occur in habitats where trawling and mining occurs, and are harvested for jewellery (Wagner *et al.* 2012; Pusceddu *et al.* 2014; Sharma 2015; Molodtsova & Opresko 2017). Conservation of black corals requires knowledge about taxonomic diversity, where species occur, and how species are related, to design interventions (e.g., marine reserves) that yield positive conservation impact (Ponder *et al.* 2001; Mace 2004; Bridge *et al.* 2016). However, little is known about the taxonomy of the group because 1) most species occur deeper than 50 m depth (Cairns 2007; Opresko 2019), making them logistically challenging to collect, 2) there are a limited number of taxonomists that specialize in black coral identification; and, 3) closely related species have few and overlapping morphological features that can be used to differentiate species,

Accepted by M. Daly: 1 Nov. 2022; published: 23 Nov. 2022

making it difficult to identify undescribed species based on morphology. Despite considerable research conducted in the Great Barrier Reef and Coral Sea, just one study has focused on the taxonomy of black corals from this region (Horowitz *et al.* 2018), and it is likely that many species remain to be described.

Herein, we describe five new black coral species collected during three recent expeditions to the Great Barrier Reef and Coral Sea, Australia. These new species are described morphologically, and molecular data of 80 black corals are used to place the new species in a systematic context within the Antipatharia. The phylogeny will also facilitate further research on the taxonomy and evolutionary history of the Order.

Materials and methods

Specimens. Specimens were collected during three expeditions to the Great Barrier Reef and Coral Sea (Fig. 1). The Voyage of the Kalinda expedition consisted of SCUBA dives along the length of the Great Barrier Reef (23.30°S to 11.13°S) from October 13 to November 2, 2019. Schmidt Ocean Institute R/V *Falkor* expedition: Seamounts, Canyons, and Reefs of the Coral Sea expedition FK200802 consisted of remotely operated vehicle (ROV) dives along the length of the Coral Sea (14.95°S to 17.43°S) from August 2 to August 30, 2020. Schmidt Ocean Institute R/V *Falkor* expedition: Northern Depths of the Great Barrier Reef expedition FK200930 consisted of ROV dives along the deep north Great Barrier Reef (24.25°S to 12.09°S) from September 30 to November 17, 2020. Together, these expeditions collected biological samples from depths from just below the surface to over 2,000 m, and the five new species from these expeditions were collected between depths of 14 and 789 m. All specimens were curated and deposited in the Queensland State collection at the Museum of Tropical Queensland (MTQ) campus of the Queensland Museum in Townsville, Australia. The reconstructed phylogeny also includes specimens from Horowitz *et al.* (2020) and specimens from museum collections across the world (see Supplementary Table 1 for specimen data).

Spine characteristics were imaged with a Hitachi TM4000 scanning electron microscope. Spine height was measured as the distance from the spine tip to the middle of the base of the spine. Polyp and branch characteristics were measured with a dissecting microscope and terminal branch diameter was measured near the base of the branch. Specimens included in this study were identified as "new to science" based on comparisons with descriptions of type material, recent taxonomic revisions, and terminology described in Opresko (2001, 2002, 2004, 2015) and Molodtsova (2006).

Accessioning of type and molecular sequences. Type material is accessioned at the Museum of Tropical Queensland, Townsville, Australia, and all molecular data were deposited in the short read archive (SRA) of the National Center for Biotechnology Information (Supplementary Table 2).

Molecular analyses. DNA extraction for most specimens followed the protocol detailed in MacIsaac *et al.* (2013) and some samples were processed using a modification of the previously optimized SDS-based extraction method (Wilson *et al.* 2002). The targeted enrichment of UCE/exon loci was carried out using the hexacoral-v2 probe design, a Hexacorallia specific bait set that was designed to maximize capture of UCE and exonic loci among hexacorals (Cowman *et al.* 2020). The hexacoral-v2 bait set includes 25,514 baits targeting 2,499 loci (1,132 UCE and 1,367 exon loci) (Cowman *et al.* 2020). The initial concentration of each extracted DNA sample was measured with a Qubit 2.0 fluorometer and sent to Arbor Biosciences (Ann Arbor, MI) for library preparation and sequencing, following details in Quattrini *et al.* (2018). Post-sequencing analyses followed Cowman *et al.* (2020) using the Phyluce software (Faircloth 2016). Raw reads were internally trimmed, assembled, matched to UCE/exon probes and aligned following the steps in Cowman *et al.* (2020), and the Phyluce online documentation (https://phyluce.readthedocs.io/en/latest/tutorial-one.html) with the notable exception that UCEs and exons were assembled and matched to separate UCE and exon probes, and then the data were combined for alignment. Individually aligned UCE/exon loci were filtered to include only those that were present in at least 50% of the samples, which were then concatenated into a single partitioned alignment. Phylogenetic relationships were reconstructed using maximum likelihood in IQtree v1.7 with 1,000 ultrafast bootstrap replicates (Minh *et al.* 2020b). ModelFinder (Kalyaanamoorthy *et al.* 2017) was used to determine the best model scheme for each UCE/exon partition to infer the evolutionary relationship of the new species to known taxa within the Order Antipatharia. Example code used for post-sequencing analyses is detailed in Supplementary Code, Section 1.

Ultrafast bootstrap support approximation, gene concordance factor and site concordance factors were estimated

across the phylogeny using IQtree. Ultrafast bootstrap approximation reduces computing time while also achieving more unbiased branch supports compared with traditional bootstrap support methods (Hoang *et al.* 2018). Gene concordance factor is defined as the proportion of gene trees that contain a given branch of the resulting phylogeny and site concordance factor is an estimation of concordance at the loci-level in the resulting phylogeny (Minh *et al.* 2020a). These metrics provide insight into agreement between gene trees and a species tree, which are used to interpret, and have greater confidence in, the tree topology (Minh *et al.* 2020a).

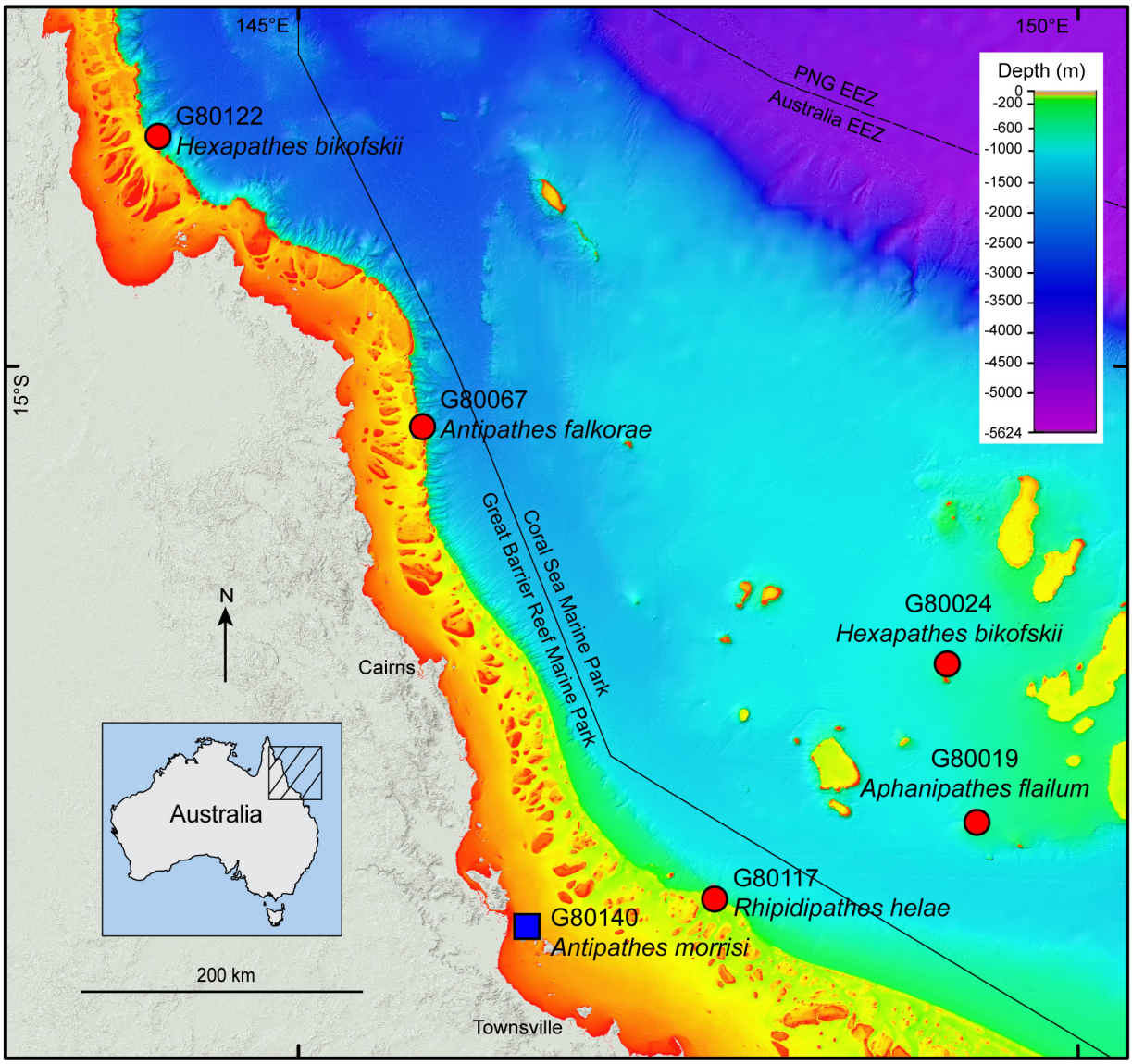

FIGURE 1. Locations where specimens were collected shown on a bathymetric surface map of the Great Barrier Reef and Coral Sea. Blue boxes represent specimens hand collected while on SCUBA, and red circles represent specimens collected via a remotely operated vehicle.

We also reconstructed a species tree using ASTRAL-III (Zhang *et al.* 2018), a multi-species coalescent method. Methods for reconstructing the species tree are as follows: IQtree v1.7 was used to create individual bootstrap trees, one for each locus post-filtering 50% taxon occupancy. Newick utilities v1.6 (Junier & Zdobnov 2010) was used to remove low support branches (< 30% bootstrap support) following the Astral III (Zhang *et al.* 2018) online tutorial (https://github.com/smirarab/ASTRAL/blob/master/astral-tutorial-template.md). TreeShrink was used to remove outlier long branches from individual gene trees and corresponding gene alignments, following the online documentation (https://github.com/uym2/TreeShrink) (Mai & Mirarab 2018). IQtree was again used to reconstruct individual bootstrap trees from the cleaned alignments, and then ASTRAL-III was used to estimate the resulting species tree (Zhang *et al.* 2018) from the individual gene trees. Example code used to make the species tree is detailed in Supplementary Code, Section 2.

Results

Molecular results. The total number of raw reads ranged from 39,887 to 12,760,452. Total number of assemblies ranged from 15,508 to 1,774,379 base pairs (average base pair lengths ranged from 272 to 1,338). The total number of matched UCE/exon loci was 2,334 with an average base pair length of 236 (ranging from 68 to 816 base pairs). The 50% taxon occupancy matrix included 1,047 loci that were concatenated into an alignment with a total length of 504,186 base pairs. Read and locus summary statistics from the UCE/exon analysis are detailed in Supplementary Table 2.

The maximum likelihood phylogeny (Fig. 2 and Supplementary Fig. 1) and species tree (Supplementary Fig. 2) are congruent at all deep nodes, and at most shallow nodes (Supplementary Figs. 1–2). The trees include all seven black coral families and place the new species in the families Antipathidae Ehrenberg, 1834, Aphanipathidae Opresko, 2004, and Cladopathidae Kinoshita, 1910.

Taxonomic results.

Family Antipathidae Ehrenberg, 1834

Genus *Antipathes* Pallas, 1766

Diagnosis (after Opresko 2019). Corallum sparsely to densely branched. Branching bushy, bramble-like, broom-like, or fan-shaped. Terminal branchlets of varying length; arranged irregularly, or bilaterally. Spines triangular or cone-shaped in lateral view; smooth or papillose; apex of spines simple or with one or more lobes or bifurcations. Polyps less than 1 mm in transverse diameter.

Type Species. *Antipathes dichotoma* Pallas, 1766

Type Locality. Mediterranean Sea

Remarks. *Antipathes dichotoma* is the type species of the Antipathidae; however, molecular studies (Bo *et al.* 2018; Brugler *et al.* 2013), including this study (Fig. 2), have found that the species is more closely related to species in the Aphanipathidae than the Antipathidae. A formal review with integrated morphological and molecular data of all species in each family is required to resolve this taxonomic issue.

Antipathes morrisi Horowitz sp. nov.
(Figs. 1–3; Supplementary Tables 1–2)

Material examined. Holotype, MTQ G80140, Australia, Great Barrier Reef, Orpheus Island, Pioneer Bay North, expedition Voyage of the Kalinda, collected on October 22, 2019, -18.5998° S, 146.4888° E, 14 m depth, collector Jeremy Horowitz.

Diagnosis. Flabellate corallum, up to ~1 cm thick; branches and terminal branchlets arranged bilaterally, or anterolaterally; overlapping, and branches anastomose. Terminal branchlets 4 to 10 mm in length, slightly curved distally, distal angles ~45 to almost 90°, 0.11 to 0.25 mm in basal diameter, spaced 2 to 5 mm apart: with a density of ~4 per cm including all rows. Spines smooth, conical, and laterally compressed, 0.085 to 0.19 mm tall. Some spines on branches possess up to four small, cone-shaped apical knobs. Four to five axial rows of spines counted in one view and four to seven spines counted in one cm in one row. Polyps 0.8 to 1 mm in transverse diameter, spaced ~0.2 mm apart, with eight to nine polyps per cm.

Description of holotype. The entire colony was 60 cm tall by 60 cm wide and 1 cm thick (Fig. 3A), but only a 28 cm tall and 20 cm wide section (MTQ G80140) was collected. The colony is branched to the fourth and rarely fifth order and has branches and terminal branchlets that are mostly distally directed and form one distinct, ~1 cm thick flabellate plane with highly anastomosing branches (Fig. 3B). Branches bilaterally arranged projecting in one plane with the smaller branchlets occurring unilaterally or bilaterally in two lateral or rarely anterolateral rows. Branches range from ~0.3 to ~1 mm in diameter excluding spine heights. Terminal branchlets are mostly 4 to 10 mm in length, have basal diameters ranging from 0.11 to 0.25 mm, and are spaced 2 to 5 mm apart on one side of a branch resulting in about 8 to 10 terminal branchlets per cm, counting terminal branches

on both sides of the branch. Branches and terminal branchlets form ~45 to almost 90° distal angles and can be almost straight or slightly curved upwards.

Spines on terminal branchlets are smooth, conical, and laterally compressed. Spines are slightly distally inclined or perpendicular to the axis with convex proximal sides, and tips curved slightly upwards (Fig. 3C). On terminal branchlets with diameters from 0.11 to 0.25 mm, polypar spine heights range from 0.12 to 0.19 mm and abpolypar spine heights range from 0.085 to 0.11 mm (Fig. 3C). On lower order branches, spines are more conical and can possess two to four small conical knobs 0.01 to 0.03 mm tall, concentrated near their apexes that are directed in the same general direction as the spine. On a section of a branch 0.22 mm in diameter, polypar spines are 0.13 mm and abpolypar spines are 0.1 mm (Fig. 3D). Four to five axial rows of spines can be counted in one view of branches and terminal branchlets and four to seven spines can be counted in one cm, in one row.

Polyps are yellow to brown in color, oblong in shape, and occur on one side of the colony, in one row. Polyps are 0.8 to 1 mm in transverse diameter and spaced ~0.2 mm apart resulting in about nine polyps per cm (Fig. 3E).

Comparative diagnosis. Twenty-one out of 67 nominal species possess flabellate planar corallums with anastomoses. Of this number, *Antipathes clathrata* Pallas, 1766 and *Antipathes tristis* (Duchassaing, 1870) have very vague original descriptions that lack sufficient taxonomic information to clearly separate these two species. All other species can be distinguished from the new species. *Antipathes delicatula* Schultze, 1896 and *Antipathes ceylonensis* (Thomson & Simpson, 1905) are more loosely branched than the new species. *Antipathes atlantica* Gray, 1857, *A. ceylonensis*, *Antipathes gracilis* Gray, 1860, *Antipathes indistincta* (van Pesch, 1914) and *Antipathes rhipidion* Pax, 1916 form only rare occasional anastomoses, whereas the new species form a densely anastomosing fan. Antipathes craticulata Opresko, 2015, *Antipathes dubia* (Brook, 1889) and *Antipathes plana* Cooper, 1909 have uniserial arrangement of terminal branchlets throughout the corallum in contrast to new species, that demonstrate characteristic biserial arrangement (Fig. 3B). The new species is also different than *A. craticulata* by having less distinctly curved branches and terminal branchlets. *Antipathes hypnoides* (Brook, 1889), *Antipathes minor* (Brook, 1889), *Antipathes sibogae* (van Pesch, 1914), and *Antipathes elegans* (Thomson & Simpson, 1905) have polyps less than 0.5 mm in transverse diameter compared with 0.8 to 1.0 mm in the new species. The new species is also different than *A. hypnoides* by having much more regularly spaced terminal branchlets and a lower density of terminal branchlets (4 per cm vs > 9 per cm). *Antipathes assimilis* (Brook, 1889), *Antipathes flabellum* Pallas, 1776 (sensu Terrano *et al.*, 2021), *Antipathes irregularis* (Thomson and Simpson, 1905), *Antipathes ternatensis* Schultze, 1896, *Antipathes zoothallus* Pax, 1932 and *Antipathes speciosa* (Brook, 1889) have rather small spine heights 0.09 mm and less, whereas the new species has polypar spines 0.12-0.19 mm and abpolypar spines 0.0085 to 0.11 mm. The new species is also different than *A. flabellum* by having branches projecting perpendicular to the colony plane, narrower distal angles (45° vs 79°), and spines that are more perpendicular.

The new species has some similarities with *Antipathes aculeata* (Brook, 1889) including fused branches and short spines with sharp and sometimes forked tips. However, the new species differs from *A. aculeata* regarding the colony thickness where the new species is only 1 cm thick because branches and terminal branchlets are arranged bilaterally forming a distinct fan-shape while *A. aculeata* forms a dense mass of branches resembling a bush. Also, the new species has a smaller terminal branchlet basal diameter compared to *A. aculeata* (0.11 to 0.25 mm vs 0.3 mm). The new species also has some features similar with *Arachnopathes ericoides* (Pallas, 1776) like fused branches and short branchlets slightly curved upwards; however, as with *A. aculeata*, the new species forms a fan while *Ar. ericoides* forms a thick and dense mass, like *A. aculeata*. Additionally, *Ar. ericoides* has spines that can be forked and inclined in different directions, including downwards, and can lack longitudinal rows (Terrana *et al.* 2020) while the new species has spines that are not forked but can be slightly multi-knobbed, not proximally directed, and form distinct longitudinal rows along branches and terminal branchlets.

This new species is phylogenetically similar to *A. falkorae* **sp. nov.** and *Ar. ericoides*; however, *A. morrisi* **sp. nov.** and *Ar. ericoides* have fused branches while *A. falkorae* **sp. nov.** does not contain any fused branches (see description below). *A. falkorae* **sp. nov.** also contains longer and straighter branches that form fronds rather than the single fan characteristic of *A. morrisi* **sp. nov.** The morphological differences are sufficient to separate the species and the phylogenetic comparison does not include holotype or topotype specimens for most species being compared with the new species in the Antipathidae, which should be done in future studies that are devoted to species delimitations.

Etymology. In recognition of the Morris Family Foundation that funds research at the Orpheus Island Research Station where the new species was first found and collected.

Distribution. Known only from the Great Barrier Reef at 14 m depth.

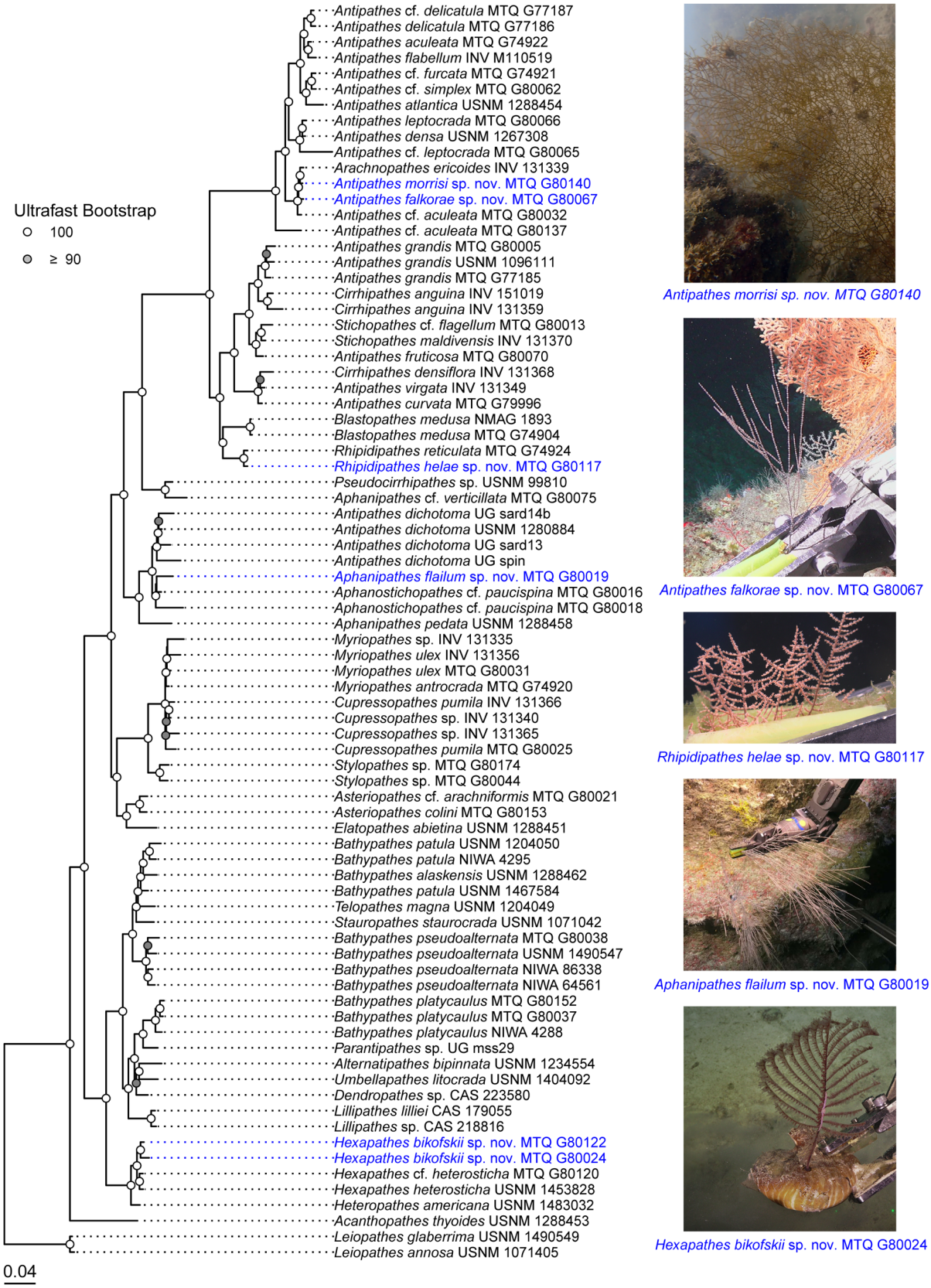

FIGURE 2. Maximum likelihood phylogeny of the Antipatharia based on a 50% complete matrix containing 1,047 loci. Taxa in blue and imaged represent species described in this study.

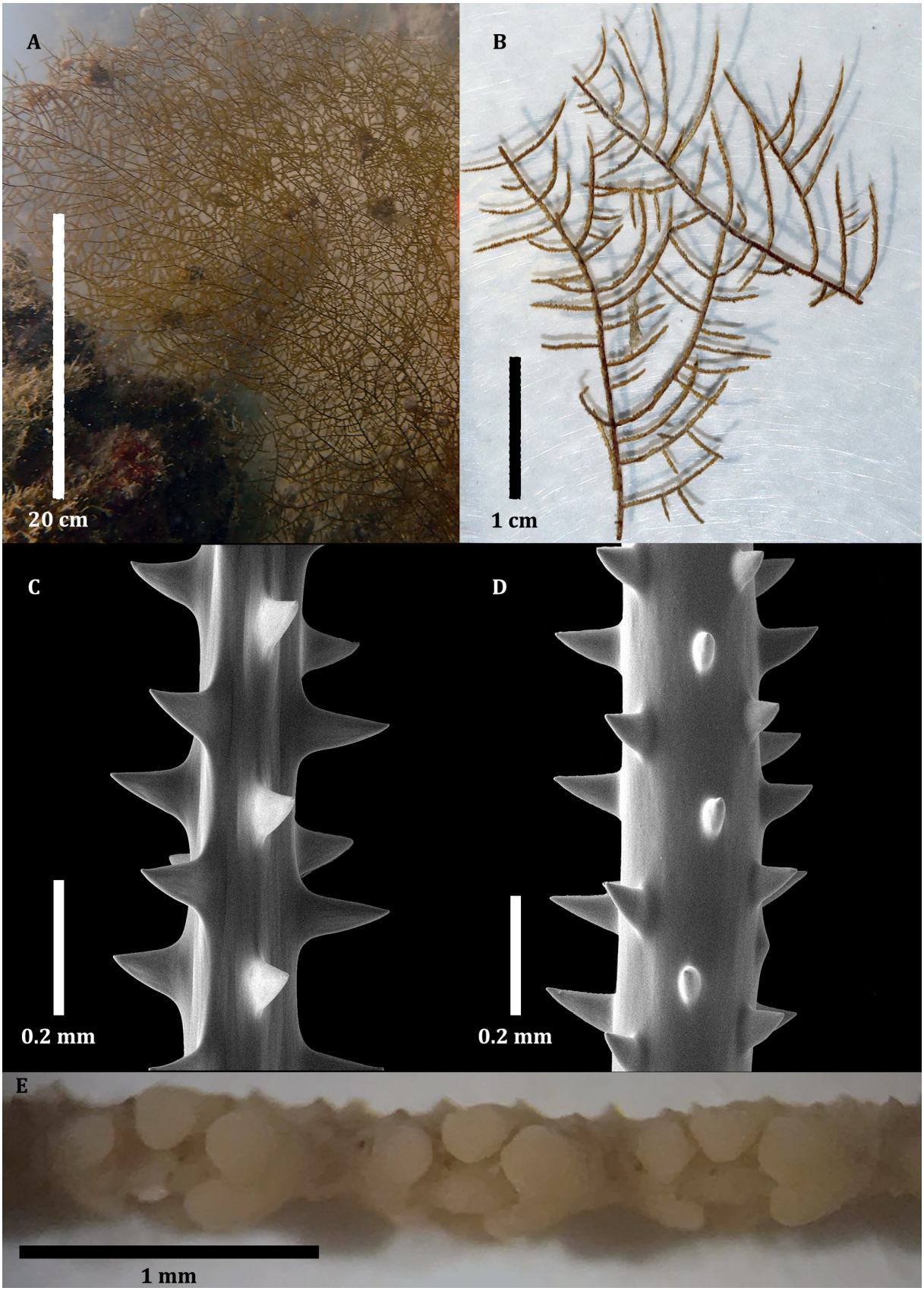

FIGURE 3. *Antipathes morrisi* **sp. nov.**: A, Holotype, G80140, *in-situ* image of colony; B, image of part of collected specimen showing branches and terminal branchlets; C, section of terminal branchlet showing polypar (right side of branchlet) and abpolypar (left side of branchlet) spines; D, section of second highest order branch showing spines; E, image of polyp row on terminal branchlet.

Antipathes falkorae **Horowitz sp. nov.**
(Figs. 1–2 and 4; Supplementary Table 1)

Material examined. Holotype, MTQ G80067, Australia, Great Barrier Reef, Ribbon Reef Canyons, Schmidt Ocean Institute R/V *Falkor*, Seamounts, Canyons, and Reefs of the Coral Sea expedition FK200802, *ROV SuBastian* dive S0385, collected on August 18, 2020, -15.3968° S, 145.7934° E, 111 m depth, collector Jeremy Horowitz.

Diagnosis. Colony fan-like, with unilateral and sparse branching mostly to the second and third order; terminal branchlets 3 to 5 cm long and curved proximally forming 45° distal branch angles. Spines conical, mostly smooth with distinct apical knobs, secondary knobs, and some papillae on the apical section of spines 0.15 to 0.17 mm tall. Four to five axial rows of spines counted in one view. Polyps 0.8 to 1 cm in transverse diameter and eight polyps per cm.

Description of holotype. Specimen is fan-like and 21 cm in height (lowermost 5 cm or more of the stem and the holdfast not collected); branched mostly to the second and rarely to the third or fourth order, with stiff and straight or slightly curved vertically directed branches (Figs. 4A–B). Distal branch angles are mostly 45°. Branching is sparse and in one plane, with mostly one and sometimes two or three branches occurring on a given lower order branch. Branching is unilateral with successive orders of branches often arising on the same side as the lower order branches. The five most basal branches are disposed on one side of the stem with subsequent branches disposed on the same side as lower order branches, while the four most apical branches occur on the opposite side of the stem and have higher order branches disposed on the same side as their direct lower order branches (Fig. 4B). The one branch between the five most basal and four most apical branches is disposed on the same side as the basal branches but has secondary branches occurring on both sides of the branch. Terminal branchlets are 3 to 5 cm in length and 0.19 to 0.2 mm in diameter near the base (Fig. 4B). The lowest portion of the stem is 0.9 mm in diameter.

Spines on a branch 0.2 mm thick or greater have polypar spines 0.15 to 0.17 mm tall and abpolypar spines 0.1 to 0.15 mm tall (Fig. 4C). On branches 0.20 mm in diameter, spines are about 0.14 mm tall (Fig. 4D), and on terminal branchlets 0.2 mm or less in diameter, spines are at most 0.13 mm tall (Fig. 4E). Spines on large (about 0.2 mm or thicker) branches have extensive apical knobbing with knobs reaching maximum heights of 0.04 mm (Fig. 4F). Where knobbing is most pronounced, spine tips flare outward (at right angles to the direction of the branch axis) and become vertically compressed with small secondary knobs occurring on primary knobs (Fig. 4G). Faint papillae can be seen on and in between well-developed knobs (Fig. 4G). Spines on terminal branchlets less than 0.2 mm in diameter have few or no apical knobs, and are smooth, triangular, slightly distally directed, laterally compressed. Four to five axial rows of spines can be counted in one view; 3.5 to 4 spines can be counted in one mm; and distances between axial rows range from ~0.3 to 0.4 mm.

Polyps are yellow to white in color, 0.8 to 1 mm in the transverse diameter with about 0.5 mm space between polyps resulting in about eight polyps in one cm (Fig. 4H).

Comparative diagnosis. *A. falkorae* **sp. nov.** is most like *Antipathes coronata* Opresko, 2019 by having straight and vertically directed branches, unilateral branching, slightly larger polypar than abpolypar spines, and apical knobs on the spines. However, the new species has more extensive apical knobbing where on a spine ~0.14 mm tall, the new species has five to six primary knobs compared to *A. coronata*, which has three knobs. The new species also has small protrusions that could be considered secondary knobs on top of primary knobs that are absent on *A. coronata*. The new species has on average a smaller terminal branchlet diameter than *A. coronata* (0.2 vs 0.3 mm); however, both species have ~5 axial spine rows visible in a lateral view. The new species also has slightly wider distal branch angles that create more of a fan shape compared to *A. coronata*. Lastly, the new species has very faint papillae on and in between primary and secondary knobs, which differs from *A. coronata* that has smooth knobs. *Antipathes elegans* Thomson & Simpson 1905 and *A. gallensis* Thomson & Simpson 1905 are also morphologically like *A. falkorae* **sp. nov.** where both have apical knobbing on the spines and faint papillae on the surface of the spines; however, the new species is different from both species by having more extensive knobbing (about six knobs per spine vs three to four in *A. elegans* and *A. gallensis*) and a presence of secondary knobs that are lacking in these other species.

This new species is phylogenetically similar to *Ar. ericoides* and *A. aculeata* (Supplementary Table 3); however, the new species does not possess fused branches while *Ar. ericoides* and *A. aculeata* have high levels of fused branches. Additionally, the specimens representing A. aculeata are not holotype or topotype specimens, which explains why they do not form a monophyletic relationship. The new species also has a low phylogenetic distance with *A. morrisi* **sp. nov.** and a feature that unites the two new species is a presence of apical knobs on the spines. However, *A. morrisi* **sp. nov.** has fused branches, unlike *A. falkorae* **sp. nov.**

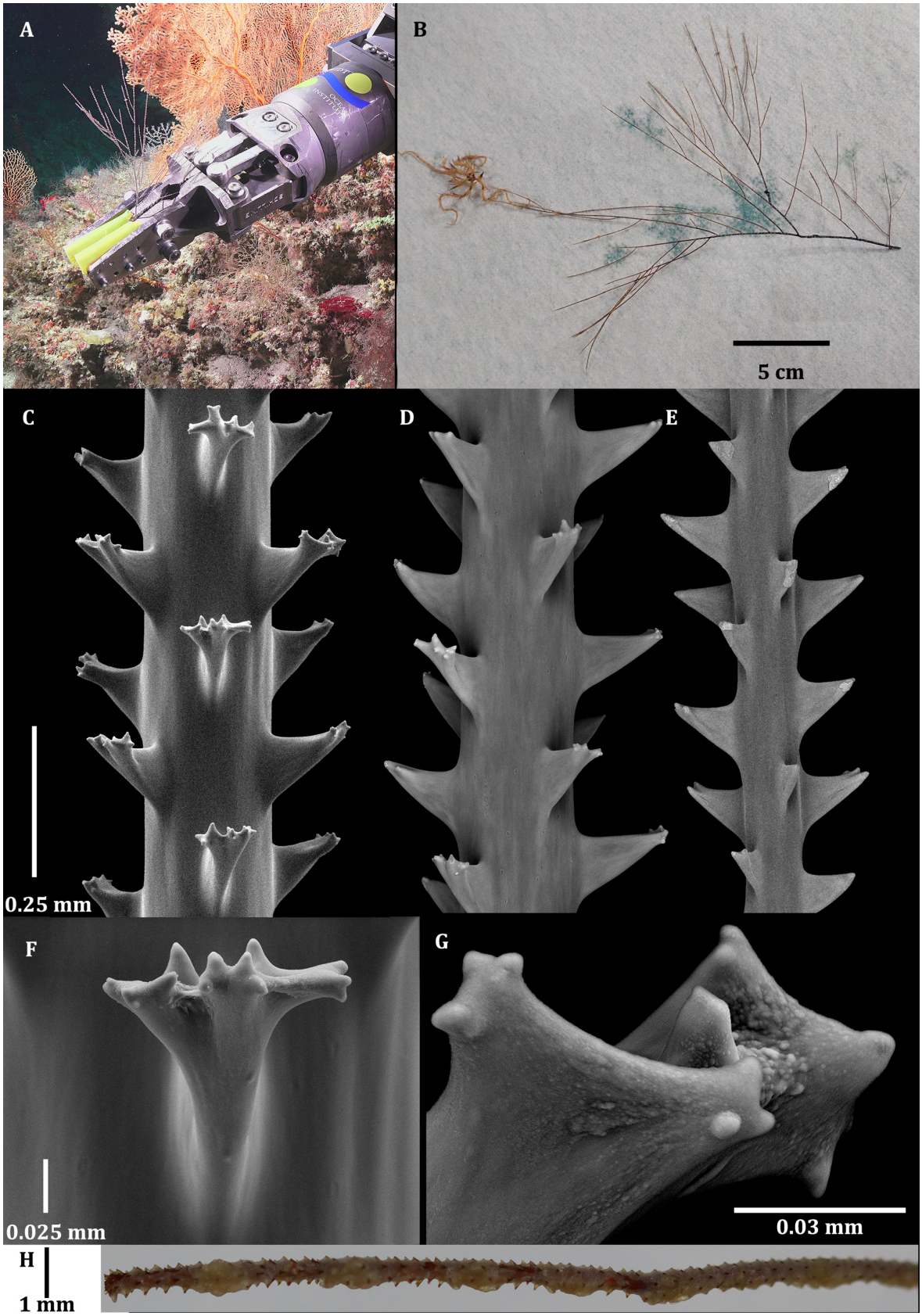

FIGURE 4. *Antipathes falkorae* **sp. nov.** Holotype, MTQ G80067: A, *in-situ* image of colony; B, image of colony showing branching pattern; C–E, sections of terminal branchlets showing spines (scale in C applicable for three subfigures); F–G, close-up of skeletal spines with knobs, secondary knobs, and papillae; H, image of polyp row on terminal branch.

Etymology. In recognition of the Schmidt Ocean Institute R/V *Falkor*, onboard which this and many other black coral species were collected from the Great Barrier Reef and Coral Sea.

Distribution. Known only from the Great Barrier Reef at 111 m depth.

Family Aphanipathidae Opresko, 2004

Genus *Rhipidipathes* Milne-Edwards & Haime, 1857

Diagnosis. Corallum flabellate; anastomosing among some branches; polypar spines acute or blunt, smooth or tuberculate; circumpolypar spines slightly larger than interpolypar spines; hypostomal spines often equal to the circumpolypar spines but may be reduced in size or absent on some portions of the corallum.

Remarks. Although *Rhipidipathes* is currently in the Aphanipathidae, previous (Brugler *et al.* 2013; Bo *et al.* 2018; Terrana *et al.* 2021) and the present study indicate that the genus is more closely related to species in the Antipathidae. The present study suggests that *Rhipidipathes* shares a lineage with the genus *Blastopathes* Horowitz, 2020 (Fig 2). Both genera have distinct morphological differences. For example, *Rhipidipathes* consists of thin branches that can fuse to create flabellate "fan-like" colonies (Opresko 2004) and *Blastopathes* consists of thick, stem-like branches that do not fuse and possess branches that sprout from clusters to create "tree-like" colonies (Horowitz *et al.* 2020). Due to the differences between these "sister" genera, their family-level relationships need to be verified.

Type Species: *Rhipidipathes reticulata* (Esper 1795)

Type Locality: East Indian Ocean

Rhipidipathes helae Horowitz sp. nov.

(Figs. 1–2 and 5; Tables 1 and Supplementary Table 1)

Material examined: MTQ G80117, Australia, Great Barrier Reef, Bowl Slide, Schmidt Ocean Institute R/V *Falkor* Northern Depths of the Great Barrier Reef expedition FK200930, *ROV SuBastian* dive S0394, collected on October 5, 2020, 18.3865° S, 147.6705° E, 119 m depth, collector Jeremy Horowitz.

Diagnosis: Corallum flabellate, branched; branches and branchlets extensively anastomosing. Terminal branchlets 0.5 to 1 cm in length and 0.08 mm in diameter, arranged bilaterally, are irregularly alternate, opposite, or subopposite, and slightly protrude from the colony plane. Spines on branches perpendicular or distally inclined. Circumpolypar spines 0.23 to 0.29 mm tall and hypostomal and interpolypar spines maximum of 0.11 mm tall. Spines on terminal branchlets are distinctly curved apically and rarely basally. Five to six axial rows of spines can be counted in one view. Surface of spines extensively tuberculated, especially from about the midpoint to the apex. Polyps roundish, 0.8 mm in transverse diameter. Interpolypar space 0.1 to 0.2 mm, with 10 polyps per cm.

Description of holotype: Colony flabellate and about 20 cm wide and 20 cm high based on estimations from *in situ* images (Figs. 5A–B). Collected sample about 7 cm wide and 9 cm tall. Longest branches are ~8 cm in length and have 0.1 cm basal diameter. Terminal branchlets are 0.5 to 1 cm in length, arranged bilaterally, and are either irregularly alternate, opposite, or subopposite. Branchlets often not strictly bilateral but slightly protrude from the general plane of the colony forming ~120° interior angles. Most terminal branchlets form ~80° distal angles and are slightly curved distally (Fig. 5B). There is extensive fusing among branches and terminal branchlets (Fig. 5C). Four anastomosing branches/branchlets can be counted in a 5 cm^2 fragment of a colony. Terminal branchlet basal diameter is 0.08 mm, distance between neighboring terminal branchlets ranges from 1 to 3 mm, and about 10 branchlets can be counted per cm of a branch, counting branches in both rows.

On a branch 0.2 mm thick, polypar spines are anisomorphic with circumpolypar spines ranging from 0.23 to 0.29 mm tall and hypostomal and interpolypar spines reduced to 0.11 mm. Abpolypar spines are uniform in height, ranging from 0.13 to 0.15 mm (Fig. 5D). Polypar spines on branches are positioned mostly perpendicular to the axis or slightly distally inclined and abpolypar spines are more distally directed than polypar spines, creating ~45° distal angles (Figs. 5D–E). Six to 10 conical and apically directed tubercles can be counted in lateral view of the polypar spines, including those on the edges (Fig. 5E) and three to six tubercles can be counted in lateral view of

abpolypar spines, with the proximal surface of all spines being mostly smooth (Figs. 5C–D). Tubercles become elongated and strongly appressed to the surface of the spine as they increase in size, reaching a maximum size of 0.03 mm (measuring the distance from the base of the tubercle to the apex of the tubercle). Tip of largest tubercles up to 0.004 mm above the spine surface (Fig. 5E). On thin branchlets (0.08 to 0.095 mm in diameter), circumpolypar spines are 0.13 mm tall, oriented perpendicular to the axis, and are distinctly curved upward (Fig. 5D, right image). On thin branchlets abpolypar spines are 0.11 mm tall, distally directed and are curved upward. On thin branchlets, a maximum of three tubercles can be counted in one lateral view of the surface of polypar and abpolypar spines, with the proximal surface of all spines being mostly smooth. On branches and terminal branchlets, five to six uneven axial rows of spines can be counted in one view.

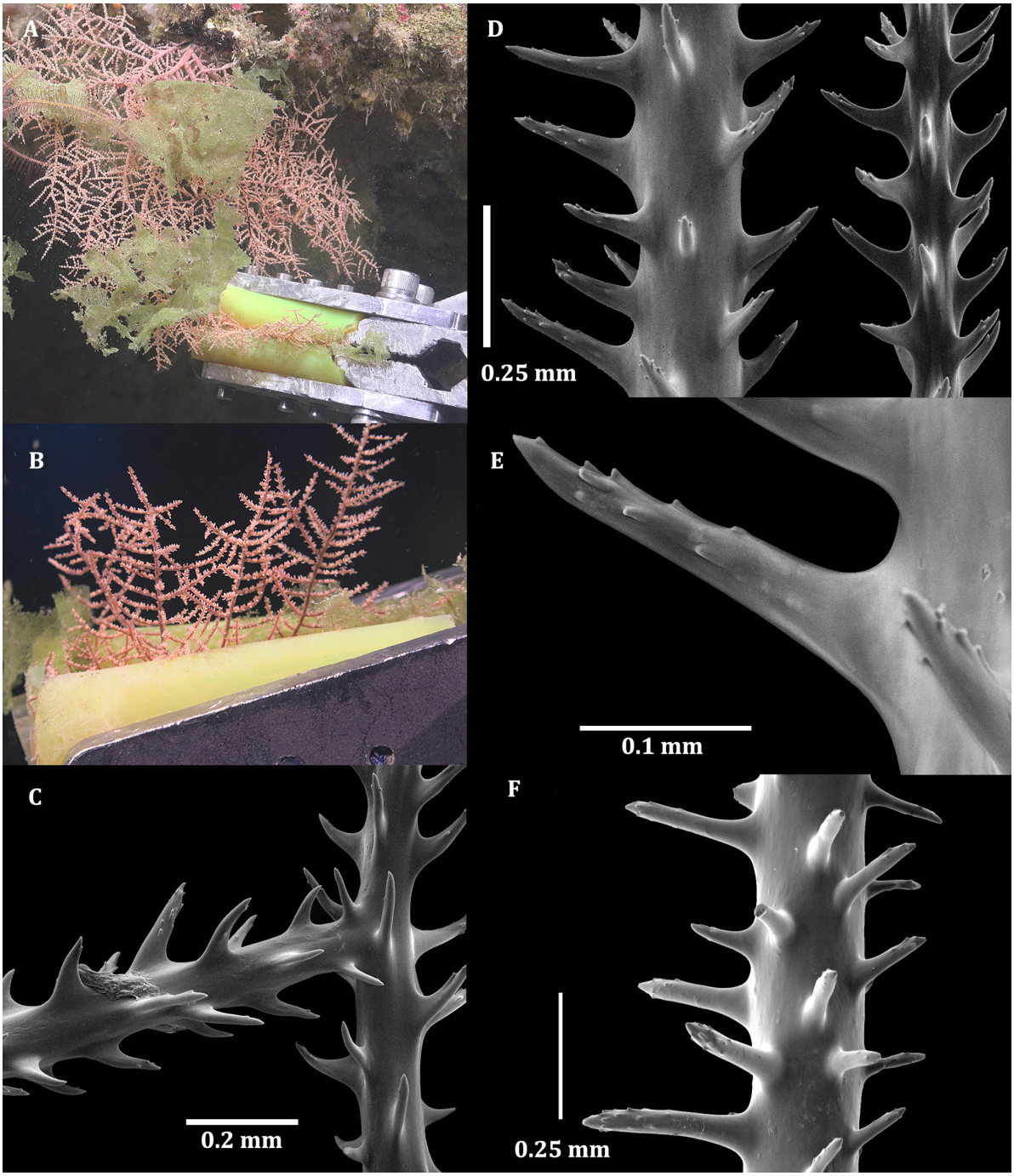

FIGURE 5. *Rhipidipathes helae* **sp. nov.**: holotype, MTQ G80117, A–E. A, *in situ* images of colony; B, collected sample; C, branches showing anastomosis; D, sections of branch (left) and terminal branchlet (right) showing curved polypar (left sides of branch and terminal branchlet) and abpolypar (right sides of branch and terminal branchlet) spines; E, skeletal spine showing tubercles; F, *Rhipidipathes reticulata (Esper),* holotype, SMF 5885*,* section of terminal branchlet showing straight spines.

TABLE 1. Comparison of *Rhipidipathes* species

Species and associated references:	*Rhipidipathes colombiana* (Opresko & Sánchez 1997)	*Rhipidipathes reticulata* (Esper 1795; Opresko & Baron-Szabo 2001)	*Rhipidipathes helae* **sp. nov.** G80117
Branch			
Longest branch (cm)	7	~10	8
Basal diameter of longest branch (cm)	> 0.3	~0.3	0.1
Arrangement of terminal branches	Bilateral, irregularly alternate	Bilateral, irregularly alternate	Bilateral, irregularly alternate
Distal angle of branches	60 to 80°	90 to 80°	80°
Terminal branchlet length (cm)	0.6 to 0.9	0.5 to 0.7	0.5 to 1
Branchlet density (per cm)	8 to 10	10	10
Relative amount of anastomosing branchlets	Limited	Extensive	Extensive
Basal diameter terminal branchlet (mm)	0.08 to 0.14	0.22	0.08
Spines (on branch 0.2 mm thick)			
Circumpolypar spine height (mm)	Up to 0.27	Up to 0.35	Up to 0.29
Hypostomal and interpolypar spines heights (mm)	Minimally reduced	Can be reduced from 0.03 to 0.04	Can be reduced to 0.11
Abpolypar spine height (mm)	0.1 to 0.11	0.11 to 0.14	0.13 to 0.15
Polypar spine distal angle	85	90 to 85	90 to 85
Abpolypar spine distal angle	45°	100 to 75°	45°
Number of tubercles in one view of polypar spine	0	3 to 7	6 to 10
Tubercles present on bottom of spine?	No	Diminished to none	Diminished to none
Tubercles present on abpolypar spines?	No	Yes	Yes
Tubercle length, tip to base (mm)	Unknown	~0.2	0.03
Tubercle distance of tip to spine surface (mm)	Unknown	Unknown	0.004
Spine orientation on terminal branchlets	Spines straight	Spines straight	Spines curved distinctly
Spine rows in one view	4 to 5	4 to 6	5 to 6
Polyp			
Shape	Slightly elongate	Unknown	Roundish
Transverse diameter of polyp (mm)	0.5 to 0.65	0.63	0.8
Polyp density (per cm)	9 to 10	10 to 11	10
Tentacle length (mm)	0.2 to 0.3		0.15

Polyps are pink, roundish with equally developed tentacles, and sagittal tentacles positioned slightly lower than lateral tentacles (Fig. 5B). On terminal branchlets and branches, polyps occur in one row; however, polyps can be arranged in several rows along thicker branches near the base of the colony. Polyps are ~0.8 mm in the transverse diameter and spaced 0.1 to 0.2 mm apart, resulting in 10 polyps per cm. Tentacles are approximated from *in situ* images to be 0.15 mm in length, when extended.

Comparative diagnosis. This is the third nominal species in the genus *Rhipidipathes*. *Rhipidipathes reticulata* (Esper 1795) and *Rhipidipathes colombiana* (Opresko & Sánchez 1997) are similar in most features (See Table 1 for comparison of three species); however, *R. colombiana* has limited anastomosing branchlets, hypostomal spines that are only minimally reduced in size, and spines with almost no tubercles while *R. reticulata* has greater anastomosing branchlets, reduced hypostomal spines, and possesses tubercles on polypar spines. The new species is morphologically and phylogenetically most similar to *R. reticulata* by having highly anastomosing branchlets and terminal branches, reduced hypostomal spines and clear presence of tubercles on spines. The new species is different from *R. reticulata* by having thinner terminal branchlets (0.08 vs 0.22 mm in the type) and has spines on terminal branchlets that are distinctly curved, mostly upward but sometimes downward, not found in *R. reticulata*. See comparison of spines on a terminal branchlet between *R. helae* **sp. nov.** (Fig. 5D, right image) that possesses upward curved spines and *R. reticulata* holotype (Fig. 5F) that possesses straight spines. Additionally, the new species has a greater number of tubercules on polypar and abpolypar spines than *R. reticulata* (six to 10 vs three to seven tubercles in one view of a polypar spine, and three to six vs zero to three tubercles in one view of an abpolypar spine).

Etymology: From the Norse, "hel", goddess of death, who is depicted wearing a headdress of curved deer antlers that resemble the distinctively curved spines of the new species.

Distribution. Known only from the Great Barrier Reef at 119 m depth.

Genus *Aphanipathes* Brook, 1889

Diagnosis. Colony sparsely to densely, irregularly branched, bushy, sometimes broom-like, with short to long, straight or curved, often ascending branches. Spines with tall and pronounced tubercles.

Type Species. *Aphanipathes sarothamnoides* Brook, 1889

Type Locality. Vanuatu

Aphanipathes flailum Horowitz sp. nov.

(Figs. 1–2 and 6; Supplementary Table 1)

Material examined. Holotype, MTQ G80019, Australia, Coral Sea, Malay Reef, expedition Schmidt Ocean Institute R/V *Falkor* Seamounts, Canyons, and Reefs of the Coral Sea expedition FK200802, *ROV SuBastian* dive S0377, collected on August 10, 2020, 17.9076° S, 149.3327° E, 210 m depth, collector Jeremy Horowitz.

Diagnosis. Colony forming fronds of long, straight uniserially arranged branches and terminal branchlets that occur mostly on abpolypar side of lower order branches. Terminal branchlets maximum of 10 cm in length, occur midway and more distal on lower order branches, and are spaced mostly 2 cm apart ranging from 0.4 to 3 cm, and have 0.2 to 0.3 mm basal diameters. Spine heights 0.09 to 0.12 mm tall with no noticeable difference in height between polypar and abpolypar spines. Spines subconical, slightly compressed on sides, and blunt apex with numerous tubercles from apex to midway down the spine or to the base. Five to six axial rows of spines can be counted in one view. Polyps round, 1.8 to 2 mm in transverse diameter, in a single row, with three to four polyps counted per cm (seven per 2 cm).

Description of holotype. This colony is upright and consists of several parallel broom-like fronds (Fig. 6A), each frond is densely branched to the sixth order with long straight and uniserially arranged branches. One 65 cm frond was collected from the colony for this study (Fig. 6B). Branches begin close to the base of the collected fragment and are uniserial, growing in one row on the upper side of each lower order branch. Branches and terminal branchlets form ~30° distal angles. Branches are long, ranging from 30 to a maximum of 37 cm in length. Terminal branchlets mostly range from 5 to 10 cm in length. Branches and terminal branchlets occur mostly on the abpolypar side of the lower order ramifications. Terminal branchlets occur from about midway along a lower order branch to the branch tip with distances between terminal branchlets being mostly 2 cm; however, in rare cases distances between terminal branchlets can be as small as 0.4 cm or as large as 3 cm. Branch diameter near the base of the collected frond is 3.2 mm in diameter, and terminal branchlet basal diameter ranges from 0.2 to 0.3 mm.

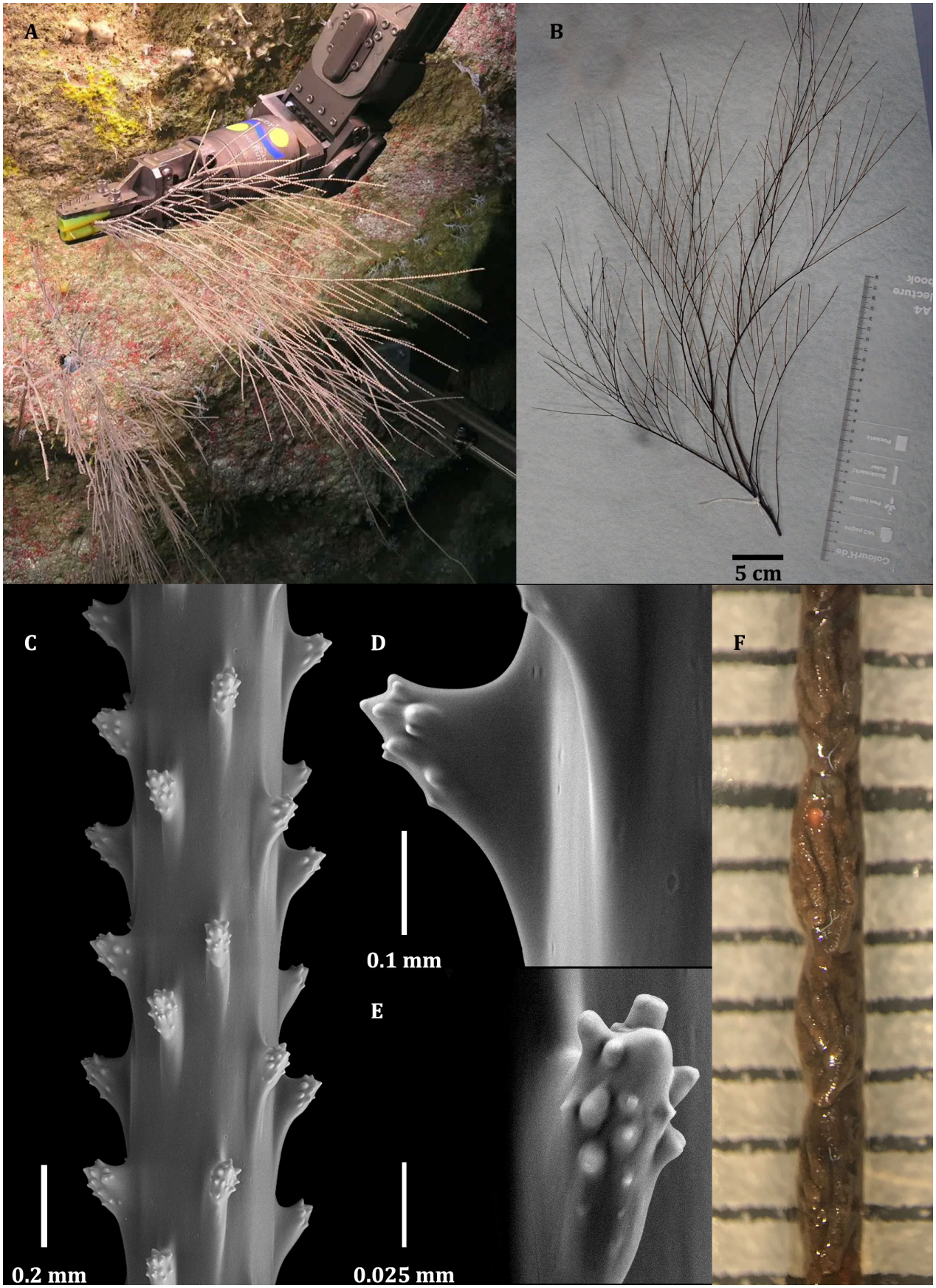

FIGURE 6. *Aphanipathes flailum* **sp. nov.** Holotype, MTQ G80019: A, *in-situ* image of colony; B, image of colony showing branching pattern; C, section of terminal branchlet showing spines with tubercles; D–E, close-up of spines showing tubercle arrangement; F, image of polyps on a branch (distances between horizontal lines represent 1 mm).

Spines on branchlets from 0.2 to 0.23 mm in diameter range from 0.09 to 0.12 mm in height and five to six axial rows of spines can be counted in a side view (Fig. 6C). Average distance between spines in one longitudinal row is 0.4 mm (Fig. 6C). Seven spines can be counted in two mm of one longitudinal row. Spines are subconical with slightly compressed sides and a blunt apex with numerous distinct tubercles (about eight to 12 in one view of one spine) covering from just around the tip of a spine in an inconsistent whorl-like fashion, to midway down the spine, or to almost the base of the spine (Fig. 6D). Tubercles are larger and more distally directed on the distal sides of spines compared to proximal sides, reaching maximum heights of 0.01 mm (Fig. 6E).

Polyps are roundish with long sagittal tentacles and distal lateral tentacles are shorter than proximal laterals in preserved state. Polyps are white (from *in-situ* video footage) to brown (after being preserved) in color, occur in one row, are mostly 1.8 to 2 mm in transverse diameter, and seven polyps can be counted in two cm (Fig. 6F).

Comparative diagnosis. This specimen bears resemblance to *Aphanipathes sarothamnoides* Brook, 1889 and *Aphanipathes pedata* (Gray 1857) in terms of their fan-like corallums with straight and distally directed branches; however, *Ap. flailum* **sp. nov.** has longer branches (25 to 30 vs 15 cm max in both *A. sarothamnoides* and *A. pedata*) and longer terminal branchlets (10 cm vs max of 4 and 3.5 cm in *A. sarothamnoides* and *A. pedata*, respectively), and a lower polyp density (3.5 to four per cm vs six per cm in *A. sarothamnoides* and no information on polyp density for the type of *A. pedata*). Terminal branchlets are also more evenly spaced along lower order branches compared to *A. pedata* that has terminal branchlets confined mostly to the distal end of the lower order branches. The new species resembles *Aphanostichopathes spiessi* (Opresko *et al.* 2021) with regards to ornamentation on the spines where both have tubercles; however, the new species has much shorter spine heights (maximum of 0.12 mm vs maximum of 0.24 mm in *Ap. spiessi*). Although *Ap. flailum* **sp. nov.** has close molecular affinity with *Aphanostichopathes cf. paucispina*, all species currently in *Aphanostichopathes* are unbranched while the new species and other species in *Aphanipathes* are branched.

Etymology: In reference to the arrangement of tubercles on the new species' subconical-shaped spines, which resembles a spiked flail, a medieval weapon.

Distribution. Known only from the Coral Sea at 210 m depth.

Family Cladopathidae Kinoshita, 1910

Genus *Hexapathes* Kinoshita, 1910

Diagnosis: Corallum simple or very sparsely branched, and pinnulate. Pinnules in two lateral rows and in one or two anterior rows. Lateral pinnules simple; anterior pinnules simple or subpinnulate. Anterior primary pinnules and subpinnules sometimes nearly as long as lateral pinnules. Spines subequal in size on primary and secondary pinnules. Polyps 3 to 6 mm in transverse diameter.

Type Species: *Hexapathes heterosticha* Kinoshita, 1910

Type Locality: Japan

***Hexapathes bikofskii* Horowitz sp. nov.**
(Figs. 1–2 and 7; Supplementary Table 1 and Table 2)

Material examined: Holotype. MTQ G80122, Australia, Great Barrier Reef, Noddy Reef, expedition Schmidt Ocean Institute R/V *Falkor* Seamounts, Canyons, and Reefs of the Coral Sea expedition 200802, *ROV Subastian* dive S0398, collected on October 15, 2020, 13.5174° S, 144.1012° E, 789 m depth, collector Jeremy Horowitz. Paratype. MTQ G80024, Australia, Coral Sea, Herald Cays, expedition Schmidt Ocean Institute R/V *Falkor* Seamounts, Canyons, and Reefs of the Coral Sea expedition 200802, *ROV SuBastian* dive S0376, collected on August 08, 2020, -16.9095° S, 149.1601° E, 638 m depth, collector Jeremy Horowitz.

Diagnosis: Colony monopodial, unbranched, and pinnulate. Pinnules arranged in two lateral rows and one anterior row. Basal-most pair of lateral pinnules subopposite, other lateral pinnules alternating. Striatum present from 1 cm above basal plate to first anterior pinnules. Lateral pinnules simple, up to 12 cm long, densities of six to 10 per 3 cm counting both rows. Anterior pinnules simple, 0.8 to 1.2 cm in length, densities of 11 to 15 per 3 cm. Polyps 4 to 6 mm in transverse diameter.

Description of holotype (G80122): Colony is monopodial and pinnulate with a slight sickle shape curvature of the stem (Fig. 7A). Grooves and ridges on the stem are present from 1 cm from the basal plate to the first anterior pinnule. Colony is 23 cm tall and 17 cm wide. Unpinnulated section of the stem is 4 cm and the pinnulated section of the stem is 19 cm (Fig. 7A). The specimen has two rows of lateral pinnules where the bottom pair of pinnules are subopposite and positioned perpendicular to the stem. Above the bottom pair of pinnules, pinnules are arranged alternately with distal angles ranging from ~80° at the bottom of the pinnulated section to ~20° at the top; with most pinnules having 45° distal angles. Lateral pinnules are curved forward and then backward so that the pinnule tips face in the opposite direction from the anterior pinnules. Lateral pinnules increase in length from the lowest pair of pinnules, which are ~8.5 cm, to midway up the pinnulated section where the longest pinnules are 12 cm, and then decrease towards the apex where the most distal pinnules are ~3 cm. Lateral pinnules are ~0.5 mm in diameter near the attachment point, and distances between pinnules in each row range from 5 to 10 mm (increasing in distance distally), resulting in 10 lateral pinnules counted near the bottom of the pinnulated section of the stem and six pinnules counted near the top of the pinnulated section, per 3 cm counting lateral pinnules in both rows. Anterior pinnules are simple, in one row and range from 0.8 to 1.5 cm in height, with most up to 1 cm in height. Distance between anterior pinnules range from 2 to 3 mm, resulting in 11 to 13 anterior pinnules counted per 3 cm.

Spines on lateral pinnules are 0.025 to 0.1 mm in height, smooth, triangular, and distally directed (Fig. 7B). Lateral pinnule spines are spaced 0.45 to 0.7 mm apart in each row, and two spines can be counted per mm in one row. Four axial rows of spines can be counted in lateral view (Fig. 7B). Spines on anterior pinnules are smooth, triangular to conical, and distally directed. Spine heights are variable, ranging from 0.04 to 0.08 mm, and the distance between spines in one row is about 0.25 mm. Three to four axial rows of spines can be counted in one view of anterior pinnules. Polyps are ~4 to 6 mm in the transverse diameter and 6 to 8 polyps counted per three cm.

Description of paratype (G80024): The colony is monopodial and pinnulate with a slight sickle shape curvature of the stem (Fig. 7C) and has two rows of distally directed lateral pinnules. Grooves and ridges are present along the stem from 1 cm above basal plate to the first anterior pinnule. Colony is 13 cm tall and 13 cm wide. The unpinnulated section of the stem is 4 cm and the pinnulated section is 9 cm in height. The lowest pair of pinnules are subopositely arranged and are positioned almost perpendicular to the axis. All other pinnules are alternating and have distal angles ranging from ~20 degrees proximally to ~80 degrees distally. Lateral pinnules increase in length from the lowest pair of pinnules, which are 4 cm, to midway up the pinnulated section where the longest pinnules range from 6.5 to 8 cm, and then decreasing towards the apex where the highest pair of pinnules are ~3 cm (Fig. 7C). Distances between pinnules range from 5 to 9 mm (increasing in distance distally), resulting in eight pinnules (near the top of the pinnulated section of stem) to 10 pinnules (near the bottom of the pinnulated section of stem) per 3 cm, counting lateral pinnules in both rows. Lateral pinnules are 0.3 mm in diameter near the attachment point. Anterior pinnules are simple, in one row with lengths ranging from 0.5 to 1 cm, with most pinnules being close to 1 cm (Fig. 7D)**.** Anterior pinnules begin from the same height on the stem as the second lowest lateral pinnules, and extend to 5 mm above the most distal lateral pinnule. Anterior pinnules are 0.18 mm in diameter near the attachment point, and distances between pinnules range from 2 to 4 mm, resulting in 13 to 15 pinnules per 3 cm. Spines on lateral pinnules 0.05 mm in height and are smooth and triangular (Fig. 7E). Lateral pinnule spines have distances between spines in one row from 0.48 to 0.7 mm and two to three spines can be counted in one mm in one row. Five axial rows of spines can be counted in one view. Spines on anterior pinnules are smooth, triangular to conical, and distally directed (Fig. 7F).

Spine heights are variable, and range from 0.02 to 0.07 mm and distances between spines in one row range from 0.32 to 0.45 mm. Three to four axial rows of spines can be counted in one view of anterior pinnules.

Polyps are in a poor state of preservation and estimated based on *in-situ* images to be reddish in color and 6 mm in the transverse diameter.

Comparative diagnosis. *H. bikofskii* **sp. nov.** is different than other species in *Hexapathes* by having only one row of simple (unpinnulated) and short (maximum of 1 cm in the new species vs maximum of 6 to 11 cm in currently described *Hexapathes* spp.) and straight anterior pinnules. See Table 2 for comparison of species in the genus.

The new species is like *H. australiensis* Opresko, 2003 and *H. alis* Molodtsova, 2006 by having just one row of anterior pinnules; however, the anterior pinnules of both species are subpinnulated while the new species has simple anterior pinnules. The new species is like *H. hivaensis* Molodtsova, 2006 and *H. heterosticha* Kinoshita, 1910 by lacking anterior subpinnules; however, both species have two or more rows of anterior pinnules while the new

species only has one row of anterior pinnules. Another difference between the new species and currently described species in the genus is the length of the unpinnulated section of the stem (ranging from 2 to 2.5 cm in described species vs 4 cm in the new species).

The new species shares other features with *H. australiensis* for the following morphometrics: 1) distance between lateral pinnules on one side of the stem (0.5 to 1 cm vs 0.4 to 1.1 cm in *H. australiensis*), both of which have spaces greater than the other three described species, and 2) the basal diameter of lateral pinnules is 0.3 to 0.5 mm in the new species and 0.5 mm in *H. australiensis*), both of which are smaller than the other three described species. The two specimens representing the new species form a clade sister to *H. heterosticha*; however, the other species in the genus have yet to be sequenced. Specimens representing species in the genus *Hexapathes* should be sequenced to further investigate morphological boundaries between species.

Etymology: In recognition of lead author's grandfather, Morton Isaiah Bikofsky, a high school teacher whose passion for science fuelled JH's interest in research.

Distribution. Known only from the Great Barrier Reef and Coral Sea from 638 to 789 m depth.

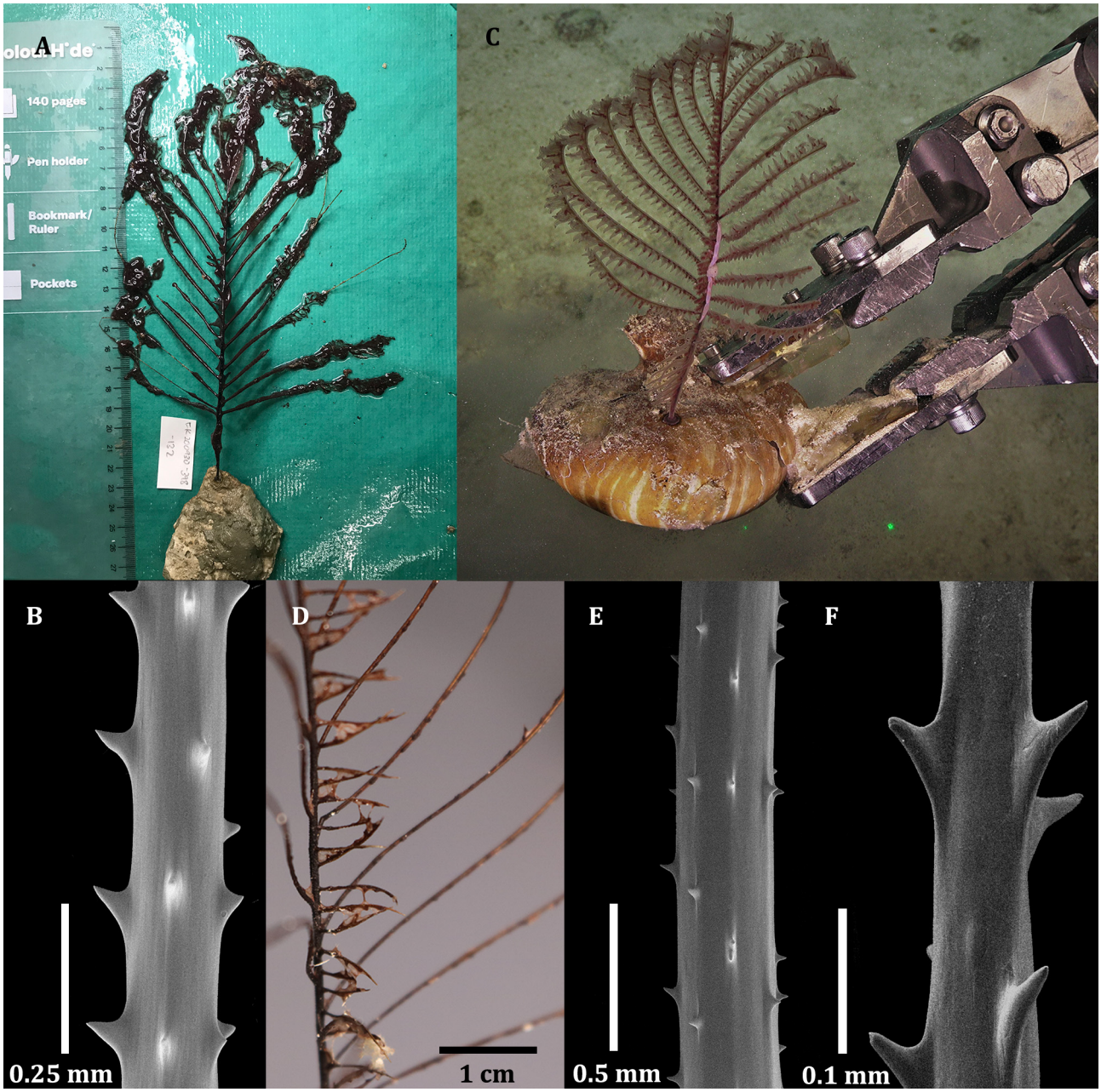

FIGURE 7. *Hexapathes bikofskii* **sp. nov.**: A, holotype, G80122, image of colony; B, holotype, G80122, section of lateral pinnule; C, paratype, G80024, *in-situ* image of colony; D, paratype, G80024, section of colony showing anterior pinnule characteristics; E, paratype, G80024, spines on section of lateral pinnule; F, paratype, G80024, spines on section of anterior pinnule.

TABLE 2. Comparison of *Hexapathes* species.

Species and associated references:	*H. heterosticha* Kinoshita, 1910	*H. australiensis* Opresko, 2003	*H. alis* Molodtsova, 2006	*H. hivaensis* Molodtsova, 2006	*H. bikofskii* **sp. nov.** *Holotype G80122*	*H. bikofskii* **sp. nov.** *Paratype G80024*
Colony						
height/width (cm)	20/19	25/7	21/20	18.5/19.5	23/17	13/13
Stem						
Basal diameter (mm)	2.0	0.9	1.8	1.8	1.0	~0.8
Unpinnulated region (cm)	2.0	2.5	2.5	2.4	4.0	4.0
Ridges and grooves at stem	N/A	Present	Present	Present, lower 2 cm of stem	From 1 cm above basal plate to first anterior pinnule	From 1 cm above basal plate to first anterior pinnule
Lateral pinnules						
Direction	Directly obliquely above	Straight, inclined distally (60°)	Curved at ends; inclined distally (30–60°)	Curved; inclined distally (20–80°)	Curved; inclined distally (20–90 degrees)	Curved; inclined distally (20–80°)
Arrangement	?	Lowermost opposite others alternate	Lowermost opposite others alternate	Lowermost opposite others alternate	Lowermost opposite others alternate	Lowermost opposite others alternate
Length (cm)	up to 14	5 up to 10.5	3–9 to 15	3.5–5 to 13–15	3–12	4–8
Distance between pinnules (mm)	2.5–6	4–11	3.5–15	2.1–4.5	5–10	5–9
Basal diameter (mm)	0.7	0.5	0.9–1.3	0.6–1.3	0.5	0.4
Anterior pinnules						
Direction	Horizontally	Basal perpendicular, upper inclined distally (70–80°)	Inclined distally (30–60°)	Perpendicularly to the stem and curved laterally	Directed horizontally	Directed horizontally
Number of rows	>1.0	1.0	1.0	>1.0	1.0	1.0
Length (cm)	up to 10	2–3 to 6	1–6.5	3–4 to 10–11	0.8–1.5	0.5–1
Subpinnules	Absent	Present	Present	Absent	Absent	Absent
Spines						
Shape	Conical, laterally compressed	Triangular to conical, laterally compressed	Triangular to conical laterally compressed	Triangular to conical laterally compressed	Triangular to conical, laterally compressed	Triangular to conical, laterally compressed
Angle	Perpendicular or inclined distally	Perpendicular or inclined distally	Perpendicular	Perpendicular or inclined distally, or proximally	Perpendicular or inclined distally	Perpendicular or inclined distally

.....continued on the next page

TABLE 2. (continued)

Species and associated references:	*H. heterosticha* Kinoshita, 1910	*H. australiensis* Opresko, 2003	*H. alis* Molodtsova, 2006	*H. hivaensis* Molodtsova, 2006	*H. bikofskii* **sp. nov.** *Holotype G80122*	*H. bikofskii* **sp. nov.** *Paratype G80024*
Size (mm)	0.05–0.10	0.08–0.12 (up to 0.14)	0.04–0.07 (up to 0.9)	0.04–0.07 (up to 0.9)	0.025–0.1	0.02–0.07
Polypar vs abpolypar spines	Larger; more inclined	Larger	No notable difference	No notable difference	Larger	No notable difference
Axial rows (lateral view)	6–9 (total?)	3–5	4–6	5–7	3–4	3–5
Density (per mm)	~2	3–4	3–5	4–5	2–4	2–4
Polyps						
Transverse diameter (mm)	5–9	3–4	2.5–6	3.1–5.3	~4–6	~6
Density (per cm)	Not reported	Not reported	Not reported	2.5 to 3	Unknown	Unknown
Sexual products	Not reported	Located at base of subpinnules	Located at base of subpinnules	Base of lateral and proximal of anterolateral	Absent	Absent

Discussion

This study demonstrates that the Great Barrier Reef and Coral Sea have greater black coral taxonomic diversity than previously thought. This is not surprising because although black corals have been collected from Australian waters and deposited in Australian museums since the late 1800s, the material is understudied due to the few taxonomists that work on Australian black corals. Continued taxonomic effort in Australia will likely lead to the discovery of more undescribed species.

This study used targeted capture techniques with high-throughput sequencing of UCEs and exonic loci, that has shown to be more informative at the genus and species-level compared to single locus markers and full mitochondrial genomes in black corals (Horowitz *et al.* 2020), hard corals (Cowman *et al.* 2020; Ramírez-Portilla *et al.* 2022), soft corals (McFadden *et al.* 2021), and more widely across the anthozoan tree of life (Quattrini *et al.* 2018, 2020). Genome reduction techniques like targeted capture methods can provide high resolution molecular datasets to aid in species delimitation (Erickson *et al.* 2021) and unravelling the evolutionary history of anthozoan lineages (McFadden *et al.* 2021; Quattrini *et al.* 2020). However, biased and incomplete species level sampling still remains an issue for species discovery and description when based solely on molecular data. This is especially true for anthozoan orders such as the Antipatharia that are still heavily reliant on a few morphological features to inform taxonomy and systematics. Herein we provide precise taxonomic assessment of specimens with reference to type material and descriptions, with phylogenetic assessment as a secondary line of evidence to highlight the systematic affinity of newly described species. Further sampling of individuals within these defined species is essential to further define their taxonomic and geographic boundaries.

Taxonomic issues can also emerge when holotype and/or topotype specimens (specimens that have features closely resembling the holotype and collected from the type locality) are absent from a phylogenetic reconstruction (Bonito *et al.* 2021). For example, the phylogenetic trees presented in this study (Fig. 2, and Supplementary Figs. 1–2) contain many Australian specimens identified to the species-level using morphological characteristics; however, most included species were not described from Australian waters. Therefore, these specimens either represent range expansions of nominal species or undescribed species that resemble nominal species morphologically, highlighting the need to include and compare original type material (where possible) or topotypes with potential undescribed species (Bonito *et al.* 2021). Doing so will provide a robust backbone phylogeny for new specimens to be compared, and allow for an estimation of phylogenetically distinctiveness between closely related species for future species descriptions. It is likely that phylogenetic distinctiveness will vary between species in different families. For example,

the two specimens representing *H. bikofskii* **sp. nov.** have a higher phylogenetic distance than the distance between *A. morrisi* **sp. nov.** and *A. falkorae* **sp. nov.** Studies have yet to formally quantify thresholds between species and how species thresholds might differ between families. Future research should utilize multispecies coalescent models to further investigate species boundaries.

Acknowledgements

We thank the Schmidt Ocean Institute R/V *Falkor* for spending most of 2020 in Australian waters surveying and sampling across the Great Barrier Reef and Coral Sea, which not only led to the findings in the current paper but also provided a treasure trove of data used in JH's PhD thesis. We thank Dr. Andrew H. Baird (AHB) for inviting JH to join the Voyage of the Kalinda, which led to the collection of one of the newly described species. We thank Julia Yun-hsuan Hung and Kristina Pahang for assistance with DNA extraction and preparation of samples for sequencing. We thank the following museums and universities for donating tissue that are included in this study: The Royal Belgian Institute of Natural Sciences, California Academy of Sciences, National Institute of Water and Atmospheric Research, National Museum of Natural History, National Museum and Art Gallery, South Australian Museum, the Tasmanian Museum and Art Gallery, and the University of Geneva. Financial support was provided to TNM by project RSF 22-24-00873. This research was funded through the ARC DECRA to PFC (DE170100516), the ARC Centre of Excellence Program (CE140100020), and ARC Centre of Excellence Discovery Grant DP180103199 awarded to AHB. Black corals from the GBR, Coral Sea, and Lord Howe were collected under the following permits: LHIMP/R/18006/01032018, G19/39364.1, G20/43974.1, and PA2020-00040-1. We also thank the two reviewers for their helpful comments and suggestions.

References

Bo, M., Barucca, M., Biscotti, M.A., Brugler, M.R., Canapa, A., Canese, S., lo Iacono, C. & Bavestrello, G. (2018) Phylogenetic relationships of Mediterranean black corals (Cnidaria: Anthozoa: Hexacorallia) and implications for classification within the order Antipatharia. *Invertebrate Systematics*, 32, 1102. https://doi.org/10.1071/is17043

Bo, M., Lavorato, A., di Camillo, C.G., Poliseno, A., Baquero, A., Bavestrello, G., Irei, Y. & Reimer, J.D. (2012) Black Coral Assemblages from Machalilla National Park (Ecuador). *Pacific Science*, 66, 63–81. https://doi.org/10.2984/66.1.4

Bonito, V.E., Baird, A.H., Bridge, T., Cowman, P.F. & Fenner, D. (2021) Types, topotypes and vouchers are the key to progress in coral taxonomy: Comment on Wepfer *et al.* (2020). *Molecular Phylogenetics and Evolution*, 159, 107104. https://doi.org/10.1016/j.ympev.2021.107104

Bridge, T.C.L., Grech, A.M. & Pressey, R.L. (2016) Factors influencing incidental representation of previously unknown conservation features in marine protected areas. *Conservation Biology*, 30, 154–165. https://doi.org/10.1111/cobi.12557

Brook, G. (1889) Report on the Antipatharia. *Report on the scientific results of the voyage of H.M.S. Challenger*, 32, 1–222.

Brugler, M.R., Opresko, D.M. & France, S.C. (2013) The evolutionary history of the order Antipatharia (Cnidaria: Anthozoa: Hexacorallia) as inferred from mitochondrial and nuclear DNA: implications for black coral taxonomy and systematics. *Zoological Journal of the Linnean Society*, 169, 312–361. https://doi.org/10.1111/zoj.12060

Cairns, S.D. (2007) Deep-water corals: An overview with special reference to diversity and distribution of deep-water scleractinian corals. *Bulletin of Marine Science*, 81, 311–322.

Cooper, C.F. (1909) Antipatharia. Reports of the Percy Sladen Trust Expedition to the Indian Ocean. *In*: *Transactions of the Linnean Society of London*, Zoology Series 2, 12, 301–323.

Cowman, P.F., Quattrini, A.M., Bridge, T.C.L., Watkins-Colwell, G.J., Fadli, N., Grinblat, M., Roberts, T.E., McFadden, C.S., Miller, D.J. & Baird, A.H. (2020) An enhanced target-enrichment bait set for Hexacorallia provides phylogenomic resolution of the staghorn corals (Acroporidae) and close relatives. *Molecular Phylogenetics and Evolution*, 153, 106944. https://doi.org/10.1016/j.ympev.2020.106944

Duchassaing, de F. (1870) s.n. *In*: *Revue des zoophytes des spongiaires des Antilles*. V. Masson, Paris, pp. 23–24.

Ehrenberg, C.G. (1834) s.n. *In*: *Die Corallenthiere des rothen Meeres, physiologisch untersucht und systematisch verzeichnet*. Abhandlung Königlichen Akademie der Wissenschaften, Berlin, pp. 153–154.

Erickson, K.L., Pentico, A., Quattrini, A.M. & McFadden, C.S. (2021) New approaches to species delimitation and population structure of anthozoans: Two case studies of octocorals using ultraconserved elements and exons. *Molecular Ecology*

Resources, 21, 78–92.
https://doi.org/10.1111/1755-0998.13241
Esper, E.J.C. (1795) *Die Pflanzenthiere in Abbildungen nach der Natur mit Farben erleuchtet nebst Beschreibungen*. in der Raspischen Buchhandlung, Nürnberg, 303 pp.
Faircloth, B.C. (2016) PHYLUCE is a software package for the analysis of conserved genomic loci. *Bioinformatics*, 32, 786–788.
https://doi.org/10.1093/bioinformatics/btv646
Gray, J.E. (1857) Synopsis of the families and genera of axiferous zoophytes or barked corals. *Proceedings of the Zoological Society of London*, 25, 278–294.
https://doi.org/10.1111/j.1096-3642.1857.tb01242.x
Gray, J.E. (1860) Notice of some new corals from Madeira discovered by JY Johnson, Esq. *The Annals and magazine of natural history; zoology, botany, and geology being a continuation of the Annals combined with Loudon and Charlesworth's Magazine of Natural History*, 6, 311.
Haime, J. & Milne-Edwards, H. (1857) *Histoire naturelle des coralliaires, ou polypes proprement dits; par H. Milne-Edwards ... Histoire naturelle des coralliaires, ou polypes proprement dits*. Roret, Paris, 326 pp.
Hoang, D.T., Chernomor, O., von Haeseler, A., Minh, B.Q. & Vinh, L.S. (2018) UFBoot2: Improving the Ultrafast Bootstrap Approximation. *Molecular Biology and Evolution*, 35, 518–522.
https://doi.org/10.1093/molbev/msx281
Horowitz, J., Brugler, M.R., Bridge, T.C.L. & Cowman, P.F. (2020) Morphological and molecular description of a new genus and species of black coral (Cnidaria: Anthozoa: Hexacorallia: Antipatharia: Antipathidae: Blastopathes) from Papua New Guinea. *Zootaxa*, 4821 (3), 553–569.
https://doi.org/10.11646/zootaxa.4821.3.7
Horowitz, J., Opresko, D.M. & Bridge, T.C.L. (2018) Black corals (Anthozoa: Antipatharia) from the deep (916 m–2542 m) Coral Sea, north-eastern Australia. *Zootaxa*, 4472 (2), 307–326.
https://doi.org/10.11646/zootaxa.4472.2.5
Junier, T. & Zdobnov, E.M. (2010) The Newick utilities: high-throughput phylogenetic tree processing in the UNIX shell. *Bioinformatics*, 26, 1669–1670.
https://doi.org/10.1093/bioinformatics/btq243
Kalyaanamoorthy, S., Minh, B.Q., Wong, T.K.F., von Haeseler, A. & Jermiin, L.S. (2017) ModelFinder: fast model selection for accurate phylogenetic estimates. *Nature methods*, 14, 587–589.
https://doi.org/10.1038/nmeth.4285
Kinoshita, K. (1910) On a New Antipatharian Hexapathes heterosticha, n. gen. and n. sp. *Annotationes Zoologicae Japonenses*, 7, 231–234.
Love, M.S., Yoklavich, M.M., Black, B.A. & Andrews, A.H. (2007) Age of black coral (Antipathes dendrochristos) colonies, with notes on associated invertebrate species. *Bulletin of Marine Science*, 80, 391–399.
Mace, G.M. (2004) The role of taxonomy in species conservation. *Philosophical Transactions of the Royal Society B: Biological Sciences*, 359, 711–719.
https://doi.org/10.1098/rstb.2003.1454
Macisaac, K.G., Best, M., Brugler, M.R., Kenchington, E.L.R., Anstey, L.J. & Jordan, T. (2013) Telopathes magna gen. nov., spec. nov. (Cnidaria: Anthozoa: Antipatharia: Schizopathidae) from deep waters off Atlantic Canada and the first molecular phylogeny of the deep-sea family Schizopathidae. *Zootaxa*, 3700, 237–58.
https://doi.org/10.11646/zootaxa.3700.2.3
Mai, U. & Mirarab, S. (2018) TreeShrink: fast and accurate detection of outlier long branches in collections of phylogenetic trees. *BMC Genomics*, 19, 272.
https://doi.org/10.1186/s12864-018-4620-2
McFadden, C.S., Quattrini, A.M., Brugler, M.R., Cowman, P.F., Dueñas, L.F., Kitahara, M.V., Paz-García, D.A., Reimer, J.D. & Rodríguez, E. (2021) Phylogenomics, Origin, and Diversification of Anthozoans (Phylum Cnidaria). *In*: Carstens, B. (Ed.), *Systematic biology*, 70, pp. 635–647.
https://doi.org/10.1093/sysbio/syaa103
Minh, B.Q., Hahn, M.W. & Lanfear, R. (2020a) New Methods to Calculate Concordance Factors for Phylogenomic Datasets. *In*: Rosenberg, M. (Ed.), *Molecular Biology and Evolution*, 37, pp. 2727–2733.
https://doi.org/10.1093/molbev/msaa106
Minh, B.Q., Schmidt, H.A., Chernomor, O., Schrempf, D., Woodhams, M.D., von Haeseler, A. & Lanfear, R. (2020b) IQ-TREE 2: New Models and Efficient Methods for Phylogenetic Inference in the Genomic Era. *In*: Teeling, E. (Ed.), *Molecular biology and evolution*, 37, pp. 1530–1534.
https://doi.org/10.1093/molbev/msaa015
Molodtsova, T. N. (2006) New species of Hexapathes Kinoshita, 1910 (Anthozoa, Antipatharia, Cladopathidae) from the South-West Pacific. *Zoosystema, Paris*, 28, 597–606.
Molodtsova, T.N. & Opresko, D.M. (2017) Black corals (Anthozoa: Antipatharia) of the Clarion-Clipperton Fracture Zone. *Marine Biodiversity*, 47, 349–365.
https://doi.org/10.1007/s12526-017-0659-6
Opresko, D.M. (2001) Revision of the Antipatharia (Cnidaria: Anthozoa). Part I. Establishment of a new family, Myriopathidae.

Zoologische Mededelingen, Leiden, 75, 343–370.
Opresko, D.M. (2002) Revision of the Antipatharia (Cnidaria: Anthozoa). Part II. Schizopathidae. *Zoologische Mededelingen, Leiden*, 76, 1–17.
Opresko, D.M. (2003) Revision of the Antipatharia (Cnidaria: Anthozoa). Part III. Cladopathidae. *Zoologische Mededelingen, Leiden*, 77, 495–536.
Opresko, D.M. (2004) Revision of the Antipatharia (Cnidaria: Anthozoa). Part IV. Establishment of a new family, Aphanipathidae. *Zoologische Mededelingen, Leiden*, 78, 1–15.
Opresko, D.M. (2015) New species of black corals (Cnidaria: Anthozoa: Antipatharia) from New Zealand and adjacent regions. *New Zealand Journal of Zoology*, 42, 145–164.
https://doi.org/10.1080/03014223.2015.1051550
Opresko, D.M. (2019) New species of black corals (Cnidaria: Anthozoa: Antipatharia) from the New Zealand region, part 2. *New Zealand Journal of Zoology*, 47, 149–186.
https://doi.org/10.1080/03014223.2019.1650783
Opresko, D.M. & Baron-Szabo, R.C. (2001) Re-descriptions of the antipatharian corals described by E. J. C. Esper with selected English translations of the original German text. *Senckenbergiana biologica*, 81, 1–21.
Opresko, D.M., Bo, M., Stein, D.P., Evankow, A., Distel, D.L. & Brugler, M.R. (2021) Description of two new genera and two new species of antipatharian corals in the family Aphanipathidae (Cnidaria: Anthozoa: Antipatharia). *Zootaxa*, 4966 (2), 161–174.
https://doi.org/10.11646/zootaxa.4966.2.4
Opresko, D.M. & Sánchez, J.A. (1997) A new species of antipatharian coral (Cnidaria: Anthozoa) from the Caribbean Coast of Colombia. *Caribbean Journal of Science*, 33, 75–81.
Pallas, P. (1766) s.n. *In*: *Elenchus zoophytorum sistens generum adumbrationes generaliores et specierum cognitarum succintas descriptiones, cum selectis auctorum synonymis*. Apud Petrum van Cleef, IIagae-Comitum the Hagae, pp. 451–451.
Pax, F. (1916) Eine neue Antipathes-Art aus Westindien. *Zoologische Jahrbücher*, Supplement 11, 433–436.
Pax, F. (1932) Beitrag zur Kenntnis der japanischen Dörnchenkorallen. *Zoologische Jahrbücher*, 63, 407–450.
Pesch, A.J. van (1914) The Antipatharia of the Siboga Expedition. *Siboga-Expeditie*, 17, 1–258.
Ponder, W.F., Carter, G.A., Flemons, P. & Chapman, R.R. (2001) Evaluation of museum collection data for use in biodiversity assessment. *Conservation Biology*, 15, 648–657.
https://doi.org/10.1046/j.1523-1739.2001.015003648.x
Pusceddu, A., Bianchelli, S., Martin, J., Puig, P., Palanques, A., Masque, P. & Danovaro, R. (2014) Chronic and intensive bottom trawling impairs deep-sea biodiversity and ecosystem functioning. *Proceedings of the National Academy of Sciences*, 111, 8861–8866.
https://doi.org/10.1073/pnas.1405454111
Quattrini, A.M., Faircloth, B.C., Dueñas, L.F., Bridge, T.C.L., Brugler, M.R., Calixto-Botía, I.F., DeLeo, D.M., Forêt, S., Herrera, S., Lee, S.M.Y., Miller, D.J., Prada, C., Rádis-Baptista, G., Ramírez-Portilla, C., Sánchez, J.A., Rodríguez, E. & McFadden, C.S. (2018) Universal target-enrichment baits for anthozoan (Cnidaria) phylogenomics: New approaches to long-standing problems. *Molecular Ecology Resources*, 18, 281–295.
https://doi.org/10.1111/1755-0998.12736
Quattrini, A.M., Rodríguez, E., Faircloth, B.C., Cowman, P.F., Brugler, M.R., Farfan, G.A., Hellberg, M.E., Kitahara, M.V., Morrison, C.L., Paz-García, D.A., Reimer, J.D. & McFadden, C.S. (2020) Palaeoclimate ocean conditions shaped the evolution of corals and their skeletons through deep time. *Nature Ecology & Evolution*, 4, 1531–1538.
https://doi.org/10.1038/s41559-020-01291-1
Ramírez-Portilla, C., Baird, A.H., Cowman, P.F., Quattrini, A.M., Harii, S., Sinniger, F. & Flot, J.F. (2022) Solving the Coral Species Delimitation Conundrum. *Systematic biology*, 71, 461–475.
https://doi.org/10.1093/sysbio/syab077
Sánchez, J.A. (1999) Black coral-octocoral distribution patterns on imelda bank, a deep-water reef, Colombia, Caribbean Sea. *Bulletin of Marine Science*, 65, 215–225.
Schultze, L. (1896) Beitrag Zur Systematik Der Antipatharien. Abhandlungen der Senckenbergischen *Naturforschenden Gesellschaft*, 23, 1–40.
Sharma, R. (2015) Environmental Issues of Deep-Sea Mining. *Procedia Earth and Planetary Science*, 11, 204–211.
https://doi.org/10.1016/j.proeps.2015.06.026
Terrana, L., Bo, M., Opresko, D.M. & Eeckhaut, I. (2020) Shallow-water black corals (Cnidaria: Anthozoa: Hexacorallia: Antipatharia) from SW Madagascar. *Zootaxa*, 4826, 1–62.
https://doi.org/10.11646/zootaxa.4826.1.1
Terrana, L., Flot, J.-F. & Eeckhaut, I. (2021) ITS1 variation among Stichopathes cf. maldivensis (Hexacorallia: Antipatharia) whip black corals unveils conspecificity and population connectivity at local and global scales across the Indo-Pacific. *Coral Reefs*, 40, 521–533.
https://doi.org/10.1007/s00338-020-02049-8
Thomson, J. & Simpson, J.J. (1905) Report on the Antipatharia collected by Prof. Herdman at Ceylon in 1902. *Supplemental Report No. XXV to the Report to the Government of Ceylon on the Pearl Oyster Fisheries of the Gulf of Manaar*, Part 4, 93–106.

Wagner, D., Luck, D.G. & Toonen, R.J. (2012) The biology and ecology of black corals (Cnidaria: Anthozoa: Hexacorallia: Antipatharia). *Advances in marine biology*, 63, 67–132.
https://doi.org/10.1016/B978-0-12-394282-1.00002-8

Wilson, K., Li, Y., Whan, V., Lehnert, S., Byrne, K., Moore, S., Ballment, E., Fayazi, Z., Swan, J., Kenway, M. & Benzie, J. (2002) Genetic mapping of the black tiger shrimp Penaeus monodon with amplified fragment length polymorphism. *Aquaculture*, 204 (3–4), 297–309.
https://doi.org/10.1016/S0044-8486(01)00842-0

WoRMS (2022) World Register of Marine Species. Available from https://www.marinespecies.org at Vliz. (accessed 30 April 2022)
https://doi.org/10.14284/170

Zhang, C., Rabiee, M., Sayyari, E. & Mirarab, S. (2018) ASTRAL-III: polynomial time species tree reconstruction from partially resolved gene trees. *BMC Bioinformatics*, 19, 153.
https://doi.org/10.1186/s12859-018-2129-y

Supplementary Tables

Supplementary Table 1. Metadata for specimens included in this study.

Museum Registration	Family	Genus	Species	Latitude	Longitude	Depth (m)	Date Collected
MTQ G74922	Antipathidae	*Antipathes*	*aculeata*	-32.42	159.11	65	15/03/2018
NMNH 1288454	Antipathidae	*Antipathes*	*atlantica*	27.84	-93.42	233	1/07/2015
MTQ G80137	Antipathidae	*Antipathes*	*cf. aculeata*	19.24	148.15	45	20/10/2019
MTQ G80032	Antipathidae	*Antipathes*	*cf. aculeata*	-16.51	147.17	119	6/08/2020
MTQ G77187	Antipathidae	*Antipathes*	*cf. delicatula*	-18.6	146.49	14	22/10/2019
MTQ G80065	Antipathidae	*Antipathes*	*cf. leptocrada*	-15.36	145.8	360	17/08/2020
MTQ G80066	Antipathidae	*Antipathes*	*cf. leptocrada*	-15.36	145.8	433	17/08/2020
MTQ G80062	Antipathidae	*Antipathes*	*cf. simplex*	21.36	150.82	40	18/10/2019
MTQ G79996	Antipathidae	*Antipathes*	*curvata*	-18.77	146.52	20	15/02/2021
MTQ G77186	Antipathidae	*Antipathes*	*delicatula*	17.47	146.41	25	23/10/2019
NMNH 1267308	Antipathidae	*Antipathes*	*densa*	34.56	171.23	297	7/06/2014
NMNH 1280884	Antipathidae	*Antipathes*	*dichotoma*	39.97	9.73	160	1/08/2013
UG SARD14b	Antipathidae	*Antipathes*	*dichotoma*	39.97	9.73	145	31/08/2013
UG SARD13	Antipathidae	*Antipathes*	*dichotoma*	39.97	9.73	144	31/08/2013
UG SPIN	Antipathidae	*Antipathes*	*dichotoma*	43.43	8.68	1,822	7/08/2018
MTQ G80067	Antipathidae	*Antipathes*	*falokorae*	-15.4	145.79	111	18/08/2020
INV M110519	Antipathidae	*Antipathes*	*flabellum*	-23.59	43.71	17	5/11/2019
MTQ G80070	Antipathidae	*Antipathes*	*fruticosa*	12.08	143.81	10	27/10/2019
MTQ G74921	Antipathidae	*Antipathes*	*furcata*	-31.58	159.11	65	15/03/2018
NMNH 1096111	Antipathidae	*Antipathes*	*grandis*	20.94	-156.76	81	26/09/2004
MTQ G80005	Antipathidae	*Antipathes*	*grandis*	-18.62	146.5	11	22/10/2019
MTQ G77185	Antipathidae	*Antipathes*	*grandis*	-20.76	160.15	26	20/10/2019
MTQ G80140	Antipathidae	*Antipathes*	*morrisi*	-18.62	146.5	14	22/10/2019
INV 131349	Antipathidae	*Antipathes*	*virgata*	-23.35	43.61	19	8/07/2016
INV 131339	Antipathidae	*Arachnopathes*	*ericoides*	-23.35	43.61	23	1/05/2019
MTQ G74904	Antipathidae	*Blastopathes*	*medusa*	-5.3	150.12	35	13/03/2019
NMAG 1893	Antipathidae	*Blastopathes*	*medusa*	-5.31	150.13	30	13/03/2019

...Continued on the next page

Supplementary Table 1. (Continued)

Museum Registration	Family	Genus	Species	Latitude	Longitude	Depth (m)	Date Collected
INV 131359	Antipathidae	*Cirrhipathes*	*anguina*	-23.5	43.72	10	7/11/2016
INV 151019	Antipathidae	*Cirrhipathes*	*anguina*	-23.35	43.62	23	24/11/2015
INV 131368	Antipathidae	*Cirrhipathes*	*densiflora*	-23.35	43.62	23	24/11/2015
NMNH 1288451	Antipathidae	*Elatopathes*	*abietina*	27.79	-93.68	130	1/07/2015
CAS 179055	Antipathidae	*Lillipathes*	*lilliei*	57.76	-173.99	897	27/06/2004
CAS 218816	Antipathidae	*Lillipathes*	*sp.*	-123.16	37.69	1,372	26/08/2016
NMNH 99810	Antipathidae	*Pseudocirrhipathes*	*sp.*	23.65	-164.52	457	15/10/1976
MTQ G80013	Antipathidae	*Stichopathes*	*cf. flagellum*	-12.63	143.54	28	16/10/2019
INV 131370	Antipathidae	*Stichopathes*	*maldivensis*	-23.35	43.61	29	25/11/2015
NMNH 1288453	Aphanipathidae	*Acanthopathes*	*thyoides*	27.79	-93.68	228	1/07/2015
MTQ G80075	Aphanipathidae	*Aphanipathes*	*cf. verticillata mauiensis*	-17.44	150.93	128	25/08/2020
MTQ G80019	Aphanipathidae	*Aphanipathes*	*flailum*	-17.91	149.33	210	10/08/2020
NMNH 1288458	Aphanipathidae	*Aphanipathes*	*pedata*	27.81	-93.69	229	1/07/2015
MTQ G80016	Aphanipathidae	*Aphanostichopathes*	*cf. paucispina*	-17.37	148.41	501	3/08/2020
MTQ G80018	Aphanipathidae	*Aphanostichopathes*	*cf. paucispina*	-15.36	145.8	377	17/08/2020
MTQ G80021	Aphanipathidae	*Asteriopathes*	*arachniformis*	-17.41	148.35	331	4/08/2020
MTQ G80153	Aphanipathidae	*Asteriopathes*	*colini*	-17.41	148.35	331	4/08/2020
MTQ G80117	Aphanipathidae	*Rhipidipathes*	*helae*	-18.39	147.67	119	5/10/2020
MTQ G74924	Aphanipathidae	*Rhipidipathes*	*reticulata*	-20.47	161.28	400	24/04/2018
NMNH 1483032	Cladopathidae	*Heteropathes*	*americana*	27.71	-92.22	401	16/12/2017
MTQ G80024	Cladopathidae	*Hexapathes*	*bikofskii*	-16.91	149.16	639	8/08/2020
MTQ G80122	Cladopathidae	*Hexapathes*	*bikofskii*	-13.52	144.1	789	15/10/2020
MTQ G80120	Cladopathidae	*Hexapathes*	*cf. heterosticha*	-17.43	150.93	441	25/08/2020
NMNH 1453828	Cladopathidae	*hexapathes*	*heterosticha*	5.86	-162.13	418	11/05/2017
NMNH 1071405	Leiopathidae	*Leiopathes*	*annosa*	27.02	-176.53	471	3/10/2003
NMNH 1490549	Leiopathidae	*Leiopathes*	*glaberrima*	30.94	-77.33	1,247	17/06/2018
MTQ G80025	Myriopathidae	*Cupressopathes*	*pumila*	-21.36	150.82	45	17/10/2019
INV 131366	Myriopathidae	*Cupressopathes*	*pumila*	-23.35	43.61	24	23/11/2015
INV 131365	Myriopathidae	*Cupressopathes*	*sp.*	-23.59	43.71	14	21/07/2016
INV 131340	Myriopathidae	*Cupressopathes*	*sp.*	-23.35	43.61	19	11/06/2018
INV 131335	Myriopathidae	*Myriopathes*	*sp.*	-23.59	43.7	17	11/05/2019
INV 131356	Myriopathidae	*Myriopathes*	*ulex*	-23.35	43.61	19	8/07/2016
MTQ G74920	Myriopathidae	*Myriopathes*	*antrocrada*	-32.42	159.11	65	15/03/2018
MTQ G80031	Myriopathidae	*Myriopathes*	*ulex*	-19.82	149.47	20	19/10/2019
NMNH 1234554	Schizopathidae	*Alternatipathes*	*bipinnata*	35.81	-122.65	2,634	30/01/2006
NMNH 1288462	Schizopathidae	*Bathypathes*	*alaskensis*	58.2	-138.98	515	6/06/2015
NMNH 1204050	Schizopathidae	*Bathypathes*	*patula*	37.46	-59.95	1,909	28/08/2005
NMNH 1467584	Schizopathidae	*Bathypathes*	*patula*	32.21	-163.62	3,017	16/09/2017

...Continued on the next page

Supplementary Table 1. (Continued)

Museum Registration	Family	Genus	Species	Latitude	Longitude	Depth (m)	Date Collected
NIWA 4295	Schizopathidae	*Bathypathes*	*patula*	-37.3	178.18	1,357	3/10/1968
NIWA 4288	Schizopathidae	*Bathypathes*	*platycaulus*	-37.54	176.97	185	13/11/2004
MTQ G80037	Schizopathidae	*Bathypathes*	*platycaulus*	-15.4	145.79	256	18/08/2020
MTQ G80152	Schizopathidae	*Bathypathes*	*platycaulus*	-17.44	150.93	216	25/08/2020
MTQ G80038	Schizopathidae	*Bathypathes*	*pseudoalternata*	-14.01	146.6	1,443	20/08/2020
NIWA 86338	Schizopathidae	*Bathypathes*	*pseudoalternata*	-34.89	179.04	1,670	24/10/2012
NMNH 1490547	Schizopathidae	*Bathypathes*	*pseudoalternata*	30.94	-77.33	1,321	17/06/2018
NIWA 64561	Schizopathidae	*Bathypathes*	*pseudoalternata*	-37.3	178.18	1,357	3/10/1968
CAS 223580	Schizopathidae	*Dendropathes*	*sp.*	n/a	n/a	n/a	n/a
UG MSS29	Schizopathidae	*Parantipathes*	*sp.*	23.65	-164.52	457	15/10/1976
NMNH 1071042	Schizopathidae	*Stauropathes*	*staurocrada*	25.7	-171.45	1,489	18/10/2003
NMNH 1204049	Schizopathidae	*Telopathes*	*magna*	37.46	-59.95	1,909	28/08/2005
NMNH 1404092	Schizopathidae	*Umbellapathes*	*sp.*	15.47	-169.07	1,528	19/09/2015
MTQ G80044	Stylopathidae	*Stylopathes*	*sp.*	-17.41	148.35	273	4/08/2020
MTQ G80174	Stylopathidae	*Stylopathes*	*sp.*	-13.52	144.1	269	15/10/2020

CAS—California Academy of Sciences
INV—Royal Belgian Institute of Natural Sciences
MTQ—Museum of Tropical Queensland
NIWA—National Institute of Water and Atmospheric Research
NMAG—National Museum and Art Gallery of Papua New Guinea
NMNH—Smithsonian Institution, National Museum of Natural History (USNM in phylogenies)
UG—Zoology Collection, University of Genova
Unk—Unknown
n/a—Not Applicable

Supplementary Table 2. Read and locus summary statistics used in the ultraconserved element and exon analysis.

Museum Registration	# of raw reads	Assemblies: total bp	Assemblies: mean length	Assemblies: min length	Assemblies: max length	Assemblies: Total loci	NCBI Bioproject	NCBI Biosample
MTQ G74922	92,553	451,917	600	231	2,041	752	PRJNA644402	SAMN15461039
NMNH 1288454	*	747,495	1,020	230	6,564	732	PRJNA588468	SAMN13244954
MTQ G80137	4,787,225	858,072	913	107	2,893	936	PRJNA644402	SAMN27734856
MTQ G80032	4,129,776	1,366,475	1,213	183	3,949	1126	PRJNA644402	SAMN27734885
MTQ G77187	3,483,231	1,408,359	1,164	153	7,263	1208	PRJNA644402	SAMN21465394
MTQ G80065	996,068	672,792	859	177	4,865	783	PRJNA644402	SAMN27734854
MTQ G80066	5,195,344	1,133,579	1,014	145	3,277	1117	PRJNA644402	SAMN27734855
MTQ G80062	2,108,684	910,036	926	152	4,481	983	PRJNA644402	SAMN27734867
MTQ G79996	780,782	598,813	569	230	2,047	1050	PRJNA644402	SAMN27734862
MTQ G77186	3,449,223	1,774,379	1,388	188	8,413	1277	PRJNA644402	SAMN27734845
NMNH 1267308	2,929,342	1,392,093	1,122	229	8,148	1241	PRJNA644402	SAMN15461034
NMNH 1280884	289,360	242,048	348	231	979	693	PRJNA644402	SAMN27734857
UG SARD14b	1,165,492	362,591	422	181	1,943	859	PRJNA644402	SAMN27734861
UG SARD13	1,664,974	461,420	503	201	2,060	921	PRJNA644402	SAMN27734860
UG SPIN	726,418	554,087	674	129	3,222	823	PRJNA644402	SAMN27734859
MTQ G80067	5,118,224	910,544	909	194	3,830	1002	PRJNA644402	SAMN27734864
INV M110519	1,142,938	1,078,424	996	151	3,581	1080	PRJNA644402	SAMN27734852
MTQ G80070	4,478,186	1,189,425	987	155	5,764	1204	PRJNA644402	SAMN27734868
MTQ G74921	44,898	389,709	513	231	1,466	758	PRJNA644402	SAMN15461036
NMNH 1096111	3,566,708	1,372,287	1,122	195	5,922	1222	PRJNA644402	SAMN21465397
MTQ G80005	2,195,812	1,030,565	1,149	149	4,558	897	PRJNA644402	SAMN27734863
MTQ G77185	3,449,223	1,416,385	1,219	133	5,082	1160	PRJNA644402	SAMN27734844
MTQ G80140	6,826,809	1,211,034	1,150	156	4,197	1053	PRJNA644402	SAMN27734858
INV 131349	3,300,922	1,580,678	1,313	118	5,294	1204	PRJNA644402	SAMN15461037
INV 131339	3,603,888	1,632,475	1,264	214	6,354	1290	PRJNA644402	SAMN15461038

...Continued on the next page

Supplementary Table 2. (Continued)

Museum Registration	# of raw reads	Assemblies: total bp	Assemblies: mean length	Assemblies: min length	Assemblies: max length	Assemblies: Total loci	NCBI Bioproject	NCBI Biosample
MTQ G74904	486,223	678,364	634	210	2,001	1070	PRJNA644402	SAMN15459017
NMAG 1893	690,212	710,410	641	230	2,337	1104	PRJNA644402	SAMN15461031
INV 131359	1,440,429	517,540	545	213	6,821	946	PRJNA644402	SAMN27734874
INV 151019	3,897,821	1,151,755	1,172	164	5,234	984	PRJNA644402	SAMN27734866
INV 131368	6,583,043	1,301,820	1,186	182	4,377	1097	PRJNA644402	SAMN27734875
NMNH 1288451	*	1,684,910	1,110	231	13,348	1517	PRJNA588468	SAMN13244956
CAS 179055	485,480	613,694	672	234	2,690	906	PRJNA644402	SAMN15461053
CAS 218816	419,483	604,897	718	234	3,904	844	PRJNA644402	SAMN15461054
NMNH 99810	39,887	15,508	272	230	407	57	PRJNA644402	SAMN27734871
MTQ G80013	771,084	953,545	947	92	5,338	1007	PRJNA644402	SAMN27734869
INV 131370	98,263	430,116	495	230	1,263	870	PRJNA644402	SAMN27734870
NMNH 1288453	*	297,448	616	231	7,073	482	PRJNA588468	SAMN13244896
MTQ G80075	2,351,831	764,980	799	128	3,382	955	PRJNA644402	SAMN27734853
MTQ G80019	997,298	893,947	890	83	3,171	1005	PRJNA644402	SAMN27734865
NMNH 1288458	*	702,092	727	229	5,707	964	PRJNA588468	SAMN13244897
MTQ G80016	1,330,929	780,009	716	199	2,767	1088	PRJNA644402	SAMN27734873
MTQ G80018	1,108,284	702,674	874	236	3,980	803	PRJNA644402	SAMN27734872
MTQ G80021	5,018,090	1,434,828	1,167	195	5,554	1230	PRJNA644402	SAMN27734881
MTQ G80153	12,760,452	1,661,542	1,269	169	3,866	1309	PRJNA644402	SAMN27734894
MTQ G80117	3,826,563	1,374,393	1,141	180	4,236	1204	PRJNA644402	SAMN27734888
MTQ G74924	778,785	1,052,313	901	237	7,644	1168	PRJNA644402	SAMN15461035
NMNH 1483032	639,504	946,616	907	207	5,072	1041	PRJNA644402	SAMN15461048
MTQ G80024	337,071	351,921	415	112	1,207	843	PRJNA644402	SAMN27734878
MTQ G80122	1,057,553	1,215,256	1,134	106	3,754	1069	PRJNA644402	SAMN27734877
MTQ G80120	4,628,627	1,494,506	1,189	183	5,122	1253	PRJNA644402	SAMN27734876

...Continued on the next page

Supplementary Table 2. (Continued)

Museum Registration	# of raw reads	Assemblies: total bp	Assemblies: mean length	Assemblies: min length	Assemblies: max length	Assemblies: Total loci	NCBI Bioproject	NCBI Biosample
NMNH 1453828	192,900	723,422	794	236	2,434	911	PRJNA644402	SAMN15461049
NMNH 1071405	1,162,282	1,191,947	1,032	219	5,313	1150	PRJNA644402	SAMN15461050
NMNH 1490549	280,165	993,502	920	191	3,032	1074	PRJNA644402	SAMN15461052
MTQ G80025	83,589	906,409	959	126	3,185	944	PRJNA644402	SAMN27734887
INV 131366	10,962,117	1,365,157	1,360	158	5,939	1006	PRJNA644402	SAMN21465400
INV 131365	280,165	472,187	530	89	1,959	887	PRJNA644402	SAMN27734882
INV 131340	5,716,350	1,542,839	1,318	131	6,053	1168	PRJNA644402	SAMN27734846
INV 131335	2,813,345	574,594	785	231	2,927	732	PRJNA644402	SAMN27734883
INV 131356	1,699,377	721,992	865	134	3,413	833	PRJNA644402	SAMN27734884
MTQ G74920	738,221	1,099,969	1,035	206	4,919	1061	PRJNA644402	SAMN15461056
MTQ G80031	4,253,233	1,135,744	1,045	154	4,652	1086	PRJNA644402	SAMN27734886
NMNH 1234554	3,195,532	772,402	898	143	7,872	859	PRJNA644402	SAMN21465392
NMNH 1288462	*	441,044	593	229	7,290	742	PRJNA588468	SAMN13244898
NMNH 1204050	3,431,436	935,044	994	143	12,531	938	PRJNA644402	SAMN27734847
NMNH 1467584	3,061,530	958,963	1,004	127	3,937	952	PRJNA644402	SAMN27734849
NIWA 4295	2,840,228	1,116,336	1,074	127	7,405	1035	PRJNA644402	SAMN27734848
NIWA 4288	6,080,999	1,272,692	1,091	233	4,370	1161	PRJNA644402	SAMN27734892
MTQ G80037	5,145,067	1,379,451	1,140	196	4,313	1208	PRJNA644402	SAMN27734891
MTQ G80152	4,253,546	1,300,955	1,168	213	3,775	1111	PRJNA644402	SAMN27734890
MTQ G80038	1,833,075	796,869	881	231	3,908	898	PRJNA644402	SAMN27734889
NIWA 86338	3,073,354	920,676	892	146	5,632	1020	PRJNA644402	SAMN21465396
NMNH 1490547	1,875,882	1,027,951	1,016	145	7,284	1002	PRJNA644402	SAMN27734850
NIWA 64561	2,940,234	1,118,575	1,059	182	8,334	1053	PRJNA644402	SAMN27734851
CAS 223580	609,560	770,863	814	241	3,796	943	PRJNA644402	SAMN15461047
UG MSS29	*	680,909	708	229	7,763	963	PRJNA588468	SAMN13244900

...Continued on the next page

Supplementary Table 2. (Continued)

Museum Registration	# of raw reads	Assemblies: total bp	Assemblies: mean length	Assemblies: min length	Assemblies: max length	Assemblies: Total loci	NCBI Bioproject	NCBI Biosample
NMNH 1071042	2,292,941	710,741	791	143	6,259	894	PRJNA644402	SAMN21465398
NMNH 1204049	2,392,755	750,357	735	163	3,586	1019	PRJNA644402	SAMN27734893
NMNH 1404092	*	572,133	773	229	14,703	740	PRJNA588468	SAMN13244902
MTQ G80044	1,018,575	944,097	1,026	230	4,360	914	PRJNA644402	SAMN27734879
MTQ G80174	1,697,560	905,359	1,044	189	4,573	865	PRJNA644402	SAMN27734880

* see Quattrini *et al.* 2020

CAS—California Academy of Sciences

INV—Royal Belgian Institute of Natural Sciences

MTQ—Museum of Tropical Queensland

NIWA—National Institute of Water and Atmospheric Research

NMAG—National Museum and Art Gallery of Papua New Guinea

NMNH—Smithsonian Institution, National Museum of Natural History (USNM in phylogenies)

UG— Zoology Collection, University of Genova

Supplementary Figures

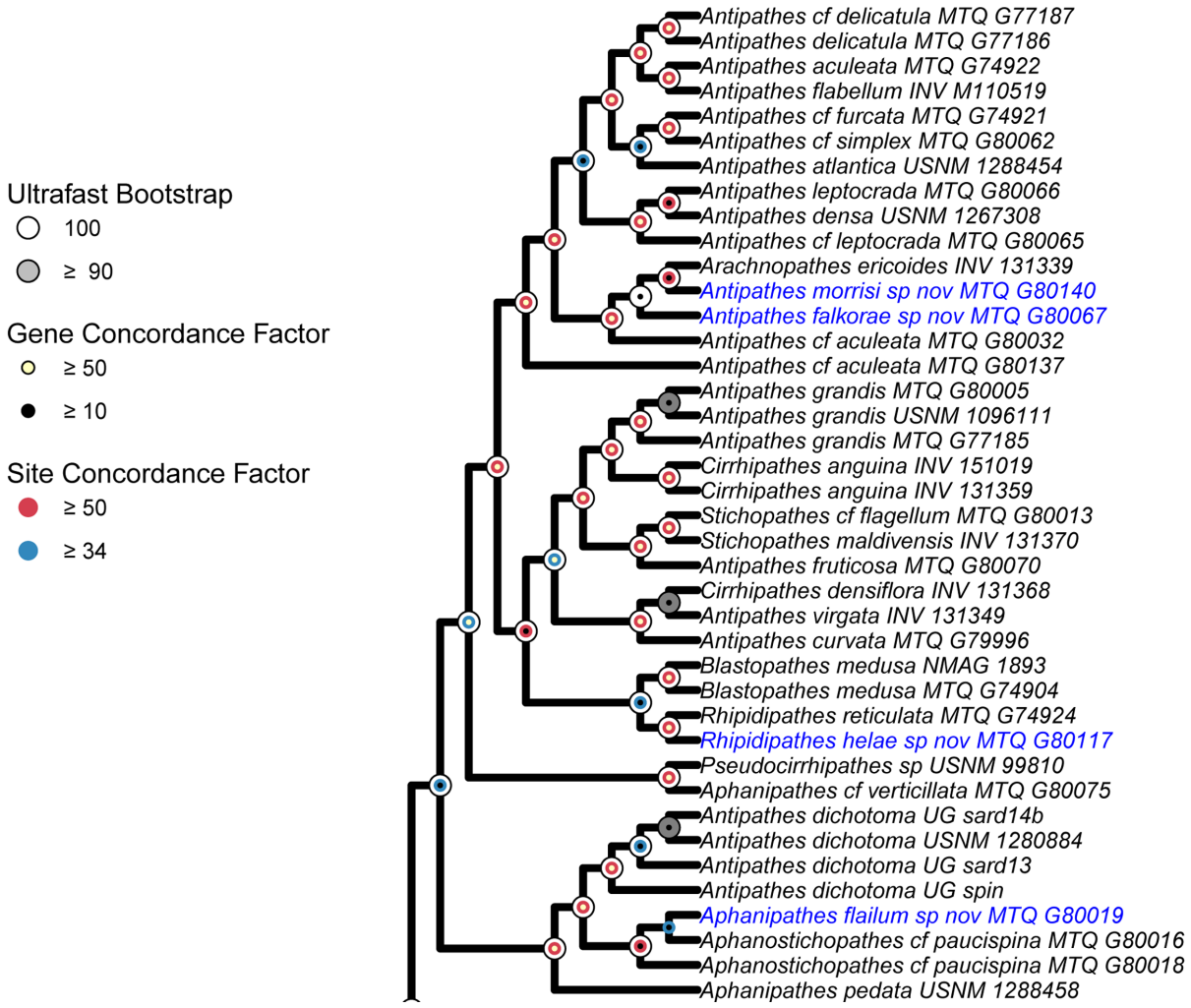

Supplementary Figure 1. Maximum likelihood cladogram of the Antipatharia based on a 50% complete matrix containing 1,047 loci. Ultrafast bootstrap value, gene concordance factor, and site concordance factor is depicted at each node. Taxa in blue represent undescribed species.

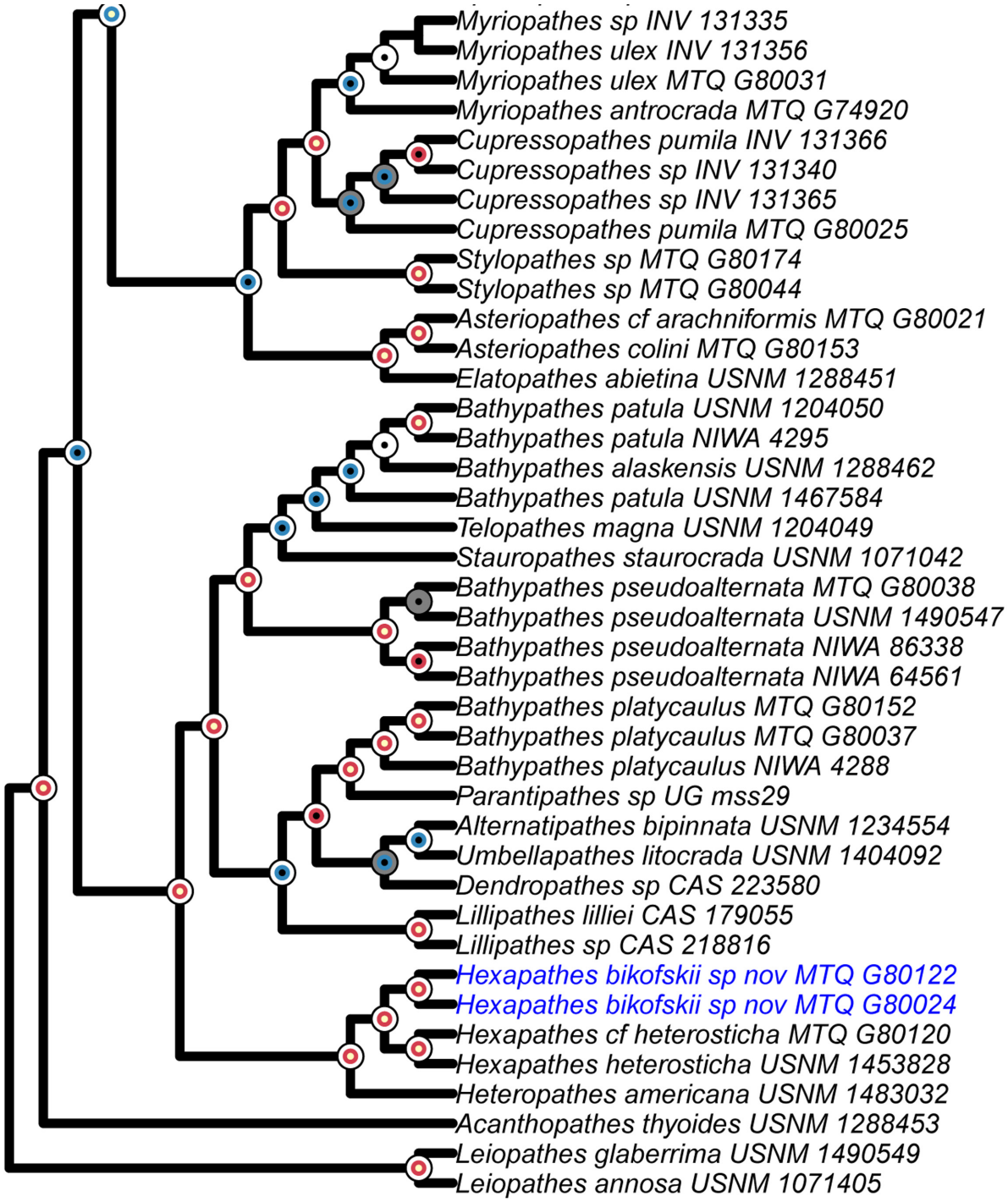

Supplementary Figure 1. Continued.

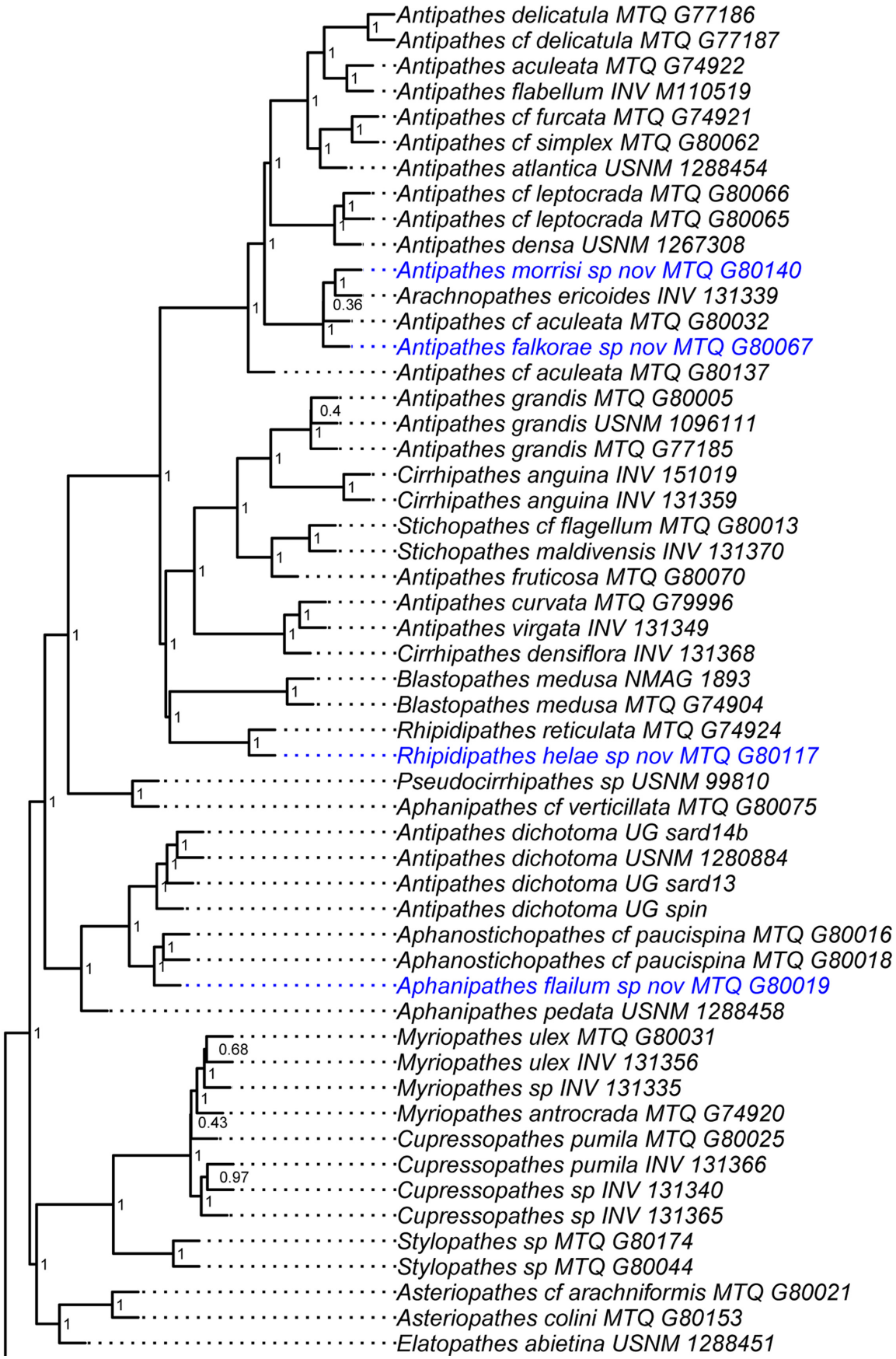

Supplementary Figure 2. Coalescent-based species phylogeny of the Antipatharia based on 1,047 gene trees using ASTRAL-III. Scale bar represents coalescent units and taxa in blue represent undescribed species.

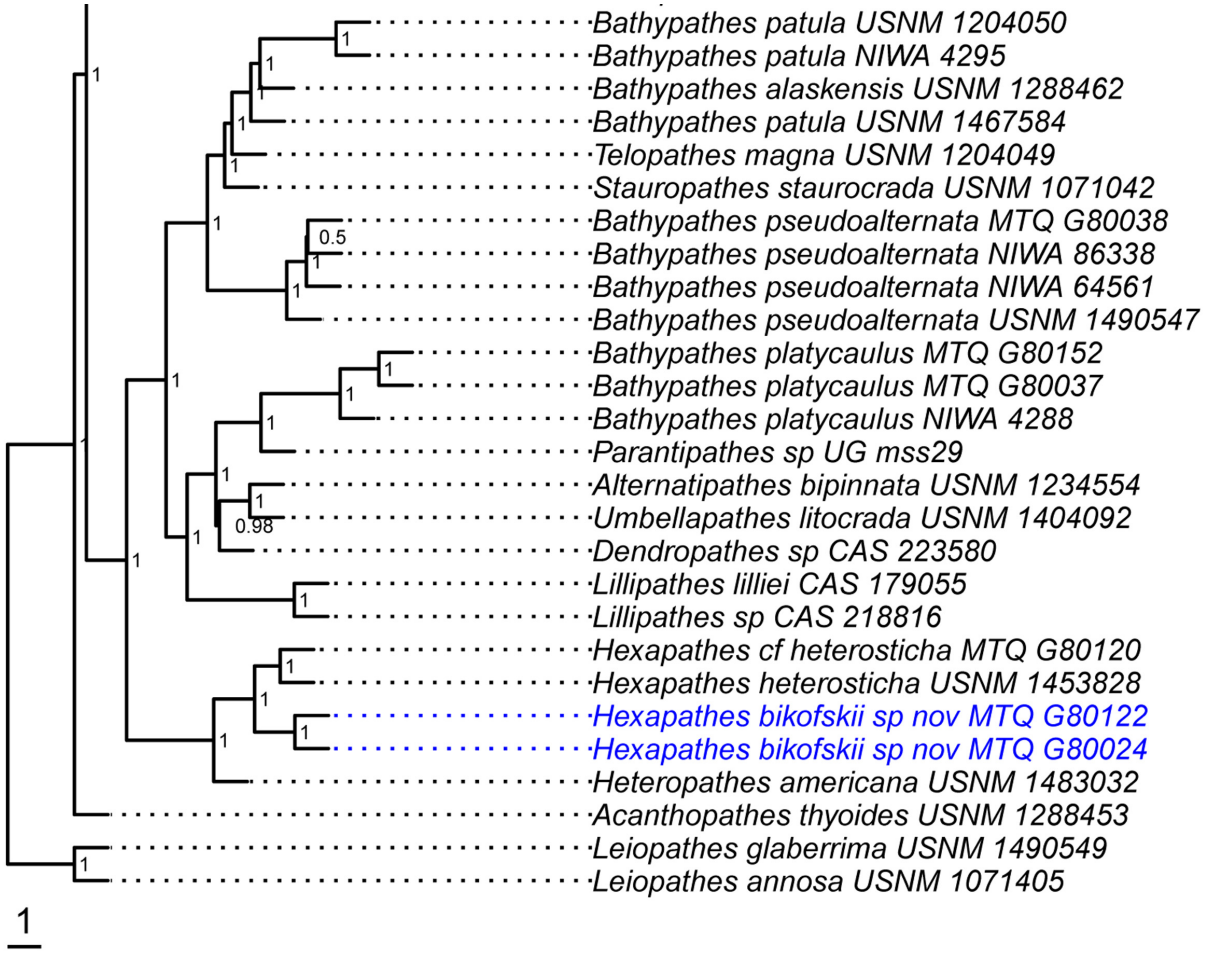

Supplementary Figure 2. Continued.

Supplementary Code

Supplementary Code. Example code used for post-sequencing analyses and tree building.

Supplementary Code

###SECTION 1

###PHYLUCE WORKFLOW (following https://phyluce.readthedocs.io/en/latest/tutorial-one.html)

#Trim and clean sequences
illumiprocessor --input rawreads --output clean-fastq --config black_coral.config --cores 48
#. /rawreads/filename example:
bc1_CTCCTAGA_L001_R1_001.fastq.gz bc2_CGTACGAA_L001_R1_001.fastq.gz
bc1_CTCCTAGA_L001_R2_001.fastq.gz bc2_CGTACGAA_L001_R2_001.fastq.gz

#Blackcoral.config example
[adapters]
i7:GATCGGAAGAGCACACGTCTGAACTCCAGTCAC*ATCTCGTATGCCGTCTTCTGCTTG
i5:AGATCGGAAGAGCGTCGTGTAGGGAAAGAGTGT*GTGTAGATCTCGGTGGTCGCCGTATCATT

[tag sequences]
i5-N501:AAGCCACA
i5-N502:AGAACGAG
i5-N503:CGTACGAA
i5-N504:CTCCTAGA

i5-N505:CTCGTCTT
i5-N506:GACGAATG
i5-N507:GCATGTCT
i5-N508:GGTCAGAT
i7-N703:AGGTTCGA
i7-N702:ACTCCATC
i7-N701:AAGAAGGC
i7-N708:GGTGTCTT
i7-N707:GCATGTCT
i7-N704:CGAAGAAC
i7-N709:TGTGACTG
i7-N705:CGAGACTA
i7-N706:GACATGGT

[tag map]
bc1_CTCCTAGA:i7-N706,i5-N504
bc2_CGTACGAA:i7-N701,i5-N503

[names]
bc1_CTCCTAGA:bc1a
bc2_CGTACGAA:bc2a

###Spades Assembly
spades.py -o /spades-assemblies-blackcoral/bc1 -1 /CLEANED_READ/bc1/split-adapter-quality-trimmed/bc1-READ1.fastq.gz -2 /CLEANED_READ/bc1/split-adapter-quality-trimmed/bc1-READ2.fastq.gz --careful --threads 40 --cov-cutoff 2;

#Example of matching uce probes to contigs, extracting and aligning them, and then running them through RAxML

phyluce_assembly_match_contigs_to_probes --contigs spades-assemblies/contigs --probes probes/hexa-v2-sclerac-subset-final-probes-uce.prbsrm.final.fasta --output uce-search-results --min-coverage 70 --min-identity 70

phyluce_assembly_get_match_counts --locus-db uce-search-results/probe.matches.sqlite --taxon-list-config taxon-set.conf --taxon-group 'bc_all' --incomplete-matrix --output taxon-sets/all/all-taxa-incomplete.conf

#Example of taxon-set.conf

[samples]
bc1
bc2

phyluce_assembly_get_fastas_from_match_counts --contigs ../../spades-assemblies/contigs --locus-db ../../uce-search-results/probe.matches.sqlite --match-count-output all-taxa-incomplete.conf --output all-taxa-incomplete.fasta --incomplete-matrix all-taxa-incomplete.incomplete --log-path log

phyluce_align_seqcap_align --fasta all-taxa-incomplete.fasta --output mafft-nexus-internal-trimmed --taxa 50 --aligner mafft --cores 12 --incomplete-matrix --output-format fasta --no-trim --log-path log

phyluce_align_get_gblocks_trimmed_alignments_from_untrimmed --alignments mafft-nexus-internal-trimmed --output mafft-nexus-internal-trimmed-gblocks --cores 12 --log log

phyluce_align_get_align_summary_data --alignments mafft-nexus-internal-trimmed-gblocks --cores 12 --log-path log --show-taxon-counts

phyluce_align_remove_locus_name_from_nexus_lines --alignments mafft-nexus-internal-trimmed-gblocks --output mafft-nexus-internal-trimmed-gblocks-clean --cores 12 --log-path log

phyluce_align_get_only_loci_with_min_taxa --alignments mafft-nexus-internal-trimmed-gblocks-clean --taxa 50 --percent 0.50 --output mafft-nexus-internal-trimmed-gblocks-clean-50p --cores 12 --log-path log

###IQTree
Inferring Species tree
iqtree2 -p /spades-taxon-sets-final/bc/mafft-nexus-internal-trimmed-gblocks-clean-50p --prefix concat.bc.i50 -B 1000 -nt 3 -m MFP+MERGE --merge-model GTR --merge-rate G -rcluster 10 --cptime 4000
Inferring gene trees

iqtree2 -S /spades-taxon-sets-final/bc/mafft-nexus-internal-trimmed-gblocks-clean-50p --prefix loci.bc.i50 -nt AUTO --cptime 4000

Gene concordance factor

iqtree2 -t concat.bc.i50.treefile --gcf loci.bc.i50.treefile -p /spades-taxon-sets-final/bc/mafft-nexus-internal-trimmed-gblocks-clean-50p --scf 100 --prefix concord.bc.i50 --cf-verbose

###SECTION 2

###SPECIES TREE METHODS

#Make gene trees as above from 50% data matrices

#Concatenate trees together into 1 file

cat uce* >out.tre

#Remove long branches from gene trees using TreeShrink (following https://github.com/uym2/TreeShrink)

run_treeshrink.py -t out.tre -o treeshr

#Prune low support (<30) branches using nw_ed

PROGRAMS/newick-utils-1.6/bin/nw_ed treeshr.tre 'i & b<=30' o > treeshr2

#Make individual gene trees (same as above) on each cleaned alignment

#Run astral (following https://github.com/smirarab/ASTRAL/blob/master/astral-tutorial-template.md)

java -jar /Astral/astral.5.6.3.jar -i treeshr2.v2.tre -o astral.all.50p.tre